NLRP3 inflammasome activation and symptom burden in *KRAS*-mutated CMML patients is reverted by IL-1 blocking therapy

Laura Hurtado-Navarro[1#], Ernesto José Cuenca-Zamora[1,2,3#], Lurdes Zamora[4], Beatriz Bellosillo[5], Esperanza Such[6], Eva Soler-Espejo[2], Helios Martínez-Banaclocha[1,7], Jesús M. Hernández-Rivas[8], Javier Marco-Ayala[2,], Laura Martínez-Alarcón[1], Lola Linares-Latorre[9], Sara García-Ávila[10], Paula Amat-Martínez[11], Teresa González[8], Montserrat Arnan[12], Helena Pomares-Marín[12], Gonzalo Carreño-Tarragona[13], Tzu Hua Chen-Liang[2], María T. Herranz[14], Carlos García-Palenciano[1,15], María Luz Morales[1,2], Andrés Jerez[1,2,3], María L Lozano[1,2,3], Raúl Teruel-Montoya[1,2,3,16], Pablo Pelegrín[‡,1,17,18,*], Francisca Ferrer-Marín[‡1,2,3,16,*]

[#]These authors contributed equally. [‡]Senior author.

[1]Biomedical Research Institute of Murcia (IMIB-Pascual Parrilla), Murcia, Spain.

[2]Hematology and Medical Oncology Department, Hospital Universitario Morales-Meseguer, Centro Regional de Hemodonación, Murcia, Spain.

[3]CIBERER CB15/00055 (U765).

[4]Myeloid Neoplasms Group, Josep Carreras Leukaemia Research Institute, ICO-Hospital Germans Trias i Pujol, Universitat Autònoma de Barcelona, Badalona, Spain.

[5]Molecular Biology Laboratory, Pathology Department, Hospital del Mar, Hospital del Mar Medical Research Institute, IMIM, Barcelona, Spain.

[6]Hematology Department, La Fe University Hospital, Valencia, Spain.

[7]Immunology Service, Hospital Universitario Virgen de la Arrixaca, Murcia, Spain.

[8]Department of Medicine, Universidad de Salamanca, Servicio de Hematología, Hospital Universitario de Salamanca. IBSAL. Salamanca, Spain.

[9]Service of Clinical Analysis and Microbiology, Fundación Instituto Valenciano de Oncología, Valencia, Spain.

[10]Department of Hematology, Hospital del Mar, Barcelona, Spain; IMIM (Hospital del Mar Medical Research Institute), Barcelona, Spain.

[11]Hematology Service, Clinic University Hospital, INCLIVA Health Research Institute, Valencia, Spain.

[12]Hematology Department. Institut Català d'Oncologia (ICO)-Hospital Duran i Reynals, IDIBELL, Barcelona, Spain.

[13]Hematology Department. Hospital Universitario 12 de Octubre, Madrid, Spain.

[14]Internal Medicine Service, Hospital Universitario Morales Meseguer, Murcia, Spain.

[15]Servicio de Anestesiología y Reanimación, Hospital Clínico Universitario Virgen de la Arrixaca, Murcia, Spain.

[16]Universidad Católica San Antonio (UCAM), Murcia, Spain.

[17]Department of Biochemistry and Molecular Biology B and Immunology, University of Murcia, Murcia, Spain.

[18]**Lead contact**: Pablo Pelegrín (pablo.pelegrin@imib.es; pablopel@um.es)

***Correspondence**: Pablo Pelegrín (pablo.pelegrin@imib.es; pablopel@um.es);

Francisca Ferrer Marín (fferrer@ucam.edu)

Twitter: @PelegrinPablo

Other Twitter: @IMIB_RMurcia; @UMU; @crh_MoralesIMIB; @UCAM; @sehh_es

Running title: Successful anti-IL-1 therapy in *KRAS* mutated CMML

Keywords: Leukemia, CMML, inflammation, KRAS, NLRP3 inflammasome, anakinra.

Abstract word count: 243

Text word count: 4,310

Number of Figures: 4

Number of Tables: 0

Data Sharing

All data from this study will be freely accessible upon request to the corresponding authors. Available raw data has been deposited at Sequence Read Archive (SRA) with BioProject PRJNA1032543.

Funding

This work was supported by grants to PP from MCIN/AEI/10.13039/501100011033 (grant PID2020-116709RB-I00), Fundación Séneca (grants 20859/PI/18, 21897/PI/22, 21081/PDC/19), the Instituto de Salud Carlos III (grants DTS21/00080, AC22/00009), and the EU Horizon 2020 project PlasticHeal (grant 965196); and by grants from the Instituto de Salud Carlos III and Fondo Europeo de Desarrollo Regional (FEDER) to FF-M (PI21/00347). LH-N was supported by the fellowship 21214/FPI/19 (Fundación Séneca, Región de Murcia, Spain). EJC-Z is supported by the training of university teachers program (FPU18/03189). MLM is supported by Next Generation EU Grant (PMP21/00052).

Ethics approval

This study was approved by the Clinical Research Ethics Committee of the Hospital Universitario Morales-Meseguer (reference no. 07/19).

Patient consent statement

All patients and donors provided written informed consent in accordance with the Declaration of Helsinki.

Summary

Chronic myelomonocytic leukemia (CMML) is frequently associated with mutations in the rat sarcoma gene (*RAS*), leading to worse prognosis. *RAS* mutations result in active RAS-GTP proteins, favoring myeloid cells proliferation and survival, and inducing the NLRP3 inflammasome together with the apoptosis-associated speck-like protein containing a caspase recruitment domain (ASC), which promote caspase-1 activation and interleukin (IL)-1β release. Here we report, in a cohort of CMML patients with mutations in *KRAS,* a constitutive activation of the NLRP3 inflammasome in monocytes, evidenced by ASC oligomerization and IL-1β release, as well as a specific inflammatory cytokine signature. Treatment of a CMML patient with a $KRAS^{G12D}$ mutation using the IL-1 receptor blocker anakinra inhibit NLRP3 inflammasome activation, reduce monocyte count, and improve the patient's clinical status, enabling a stem cell transplant. This reveals a basal inflammasome activation in *RAS*-mutated CMML patients and suggests potential therapeutic applications of NLRP3 and IL-1 blockers.

INTRODUCTION

Chronic myelomonocytic leukemia (CMML) is a rare, age-related myeloid neoplasm with overlapping features of myelodysplastic syndromes and myeloproliferative neoplasms (MDS/MPN). It is characterized by sustained clonal monocytosis, ineffective hematopoiesis and an inherent risk of transformation to secondary acute myeloid leukemia (sAML)[1,2]. Cytogenetic alterations (present in only 20-30% of patients) or molecular clonal abnormalities are supportive criteria for diagnosis[1–4]. Based on peripheral blood (PB) white blood cell (WBC) count, both the International Consensus Classification[1] and the new (5th) WHO edition of myeloid neoplasms[2] formally recognize two subtypes: myelodysplastic (CMML-MD) and myeloproliferative (CMML-MP), with a WBC count < or ≥ 13 x 10^9/L, respectively. Compared to the CMML-MD subtype, the CMML-MP subtype confers a worse prognosis[5–7].

Importantly, CMML-MP is enriched in mutations in rat sarcoma GTPase (*RAS*) oncogenes such as *NRAS* (neuroblastoma *RAS*) and/or *KRAS* (Kirsten *RAS*)[5]. The RAS/RAF/MEK/ERK signaling pathway regulates key cellular functions such as cell proliferation, differentiation, and survival[8]. It has recently been shown that *RAS* mutations not only act through its canonical signaling pathway but also contribute to malignancy through activation of NLRP3 (Nucleotide-binding domain leucine-rich repeat containing with pyrin domain-containing 3)[9]. The NLRP3 inflammasome is a multiprotein complex that is activated in response to different pathogen-associated signals and endogenous damage; its activation leads to recruitment of an adaptor protein apoptosis-associated speck-like protein containing a caspase recruitment domain (ASC) which oligomerizes to form long filaments culminating in a large intracellular oligomer called ASC 'speck'. Pro-caspase-1 then binds to the oligomeric ASC filaments via homotypic interactions between the caspase recruitment domain (CARD), leading to their activation and consequently to

the processing and release of the proinflammatory cytokines interleukin IL-1β and IL-18 via gasdermin D-dependent plasma membrane permeabilization. Gasdermin D pore formation in the plasma membrane could be repaired by recruiting the endosomal sorting complexes required for transport mechanisms and result in a living hyperactive state of the cell, however, if gasdermin D pores could not be repaired the cell undergoes pyroptotic cell death[10].

Pyroptosis also leads to the release of ASC specks into the extracellular space, where they could amplify the inflammatory response[11–13]. The initial step of NLRP3 activation requires, among others, reactive oxygen species (ROS) production[14,15]. *KRAS* mutation leads to activation of RAC1 (Ras-related C3 botulinum toxin substrate 1), and ROS production, which favors NLRP3 inflammasome activation[9]. Based on animal models, a therapeutic approach consisting of immune modulation through blockade of the NLRP3/IL-1β axis has been proposed for CMML with a *KRAS* mutation[9]. Clinical trials with novel NLRP3 blockers are starting to be developed to treat inflammatory diseases[16]; but so far, the only drugs approved for treating NLRP3-related diseases target IL-1 through either blocking antibodies (canakinumab) or recombinant IL-1 receptor antagonists (anakinra). Data regarding the efficacy of using these inhibitors in hematologic malignancies are limited to mouse models and *in vitro* studies[9,17,18]. This is not a minor issue, as allogeneic hematopoietic stem cell transplantation (HSCT), the only curative treatment available[19], is rarely feasible for most CMML patients[20,21]. In addition, hypomethylating agents, the only approved therapy, have dismal response rates in the MP subtype[22].

Our aim was to study the mechanisms underlying NLRP3/IL-1β axis disruption and *RAS* mutations in patients with CMML and to analyze the clinical efficacy of IL-1β inhibitors in this setting. We demonstrate in a cohort of CMML $KRAS^{mut}$ a basal oligomerization of

the inflammasome and that even when NLRP3 inhibition or IL-1R blockade could not eliminate the malignant clone, this therapy was able to reduce the inflammatory symptoms in a CMML *KRAS*^{G12D} patient and facilitate clinical improvement, making potentially curative treatments, such as HSCT, possible.

RESULTS

The index patient

The index patient was a hypertensive male diagnosed in July 2020, at the age of 54 years, of a high-risk CMML-2, MP variant with a *KRAS*^{G12D} mutation. At the age of 45 years, he had suffered from revascularized ischemic heart disease. His medical history was characterized by recurrent episodes of cellulitis (n=3), and one episode (in 2019) of effusive-constrictive pericarditis accompanied by pleural effusion and right heart failure. He presented persistent monocytosis, anemia, thrombocytopenia, and splenomegaly. Cytogenetic, fluorescence *in situ* hybridization (-5/del5q and -7/del7q, PDGFR alpha/beta and FGFR-1) and molecular (*JAK2*, *CALR*, *MPL*, *ASXL1*, *KIT* and *BCR::ABL1*) studies found no relevant findings. Sequencing by gene panel related to myeloid disorders, however, revealed the presence of the c.35G>A, p.G12D variant in the *KRAS* gene (allelic burden of 48.9%). A PB smear and bone marrow (BM) aspirate/biopsy showed atypical monocytes, marked dysplastic features and 11% of immature elements between myeloblasts, monoblasts and promonocytes (**Figure S1A**), with CD123 positive cell clusters (**Figure S1B**), findings compatible with the diagnosis of *KRAS*^{G12D} CMML-2 (based on the percentage of blasts and promonocytes in BM) (**Table S1**, patient #1). Although the morphological examination of the BM ruled out the presence of vacuoles in myeloid and erythroid precursor cells, as it has been recently described that some CMML co-occur with VEXAS syndrome[23], exome sequencing data were used to discard the presence of mutations in *UBA1*.

At that time, the patient presented constitutional syndrome and treatment with low-dose corticosteroids and subsequently colchicine for constrictive pleuropericarditis were started. Unfortunately, colchicine treatment was discontinued early due to digestive intolerance. Between October and November 2020, the patient suffered new episodes of

autoinflammation -orchiepididymitis, pneumonitis, and cellulitis (**Figure 1A**). A study of inflammatory parameters was performed afterwards, showing that IL-1β release from PB mononuclear cells (PBMCs) was elevated compared to healthy donors (**Figure 1B**).

Blockade of IL-1R with anakinra as a bridge therapy to allogeneic HSCT

Given the impossibility of performing HSCT at that time (second wave of the coronavirus pandemic, COVID-19), 5 months after diagnosis, among the available anti-inflammatory drugs, anakinra (100 mg/day subcutaneous, s.c.) was chosen because of its direct inhibitory action on the IL-1 receptor. Treatment was started with good clinical response (weight gain), monocyte count stabilization (**Figure 1C**) and no toxicity. The patient remained clinically stable for four months, until he presented new episodes of autoinflammation with orchiepididymitis (**Figure 1D**), cellulitis and bilateral pneumonitis (**Figure 1E, top panel**). Empirical antibiotic treatment was started, and anakinra discontinued. Due to worsening pulmonary opacities (**Figure 1E, bottom panel**) and severe right heart failure, he required hospital admission. Despite intensive diuretic treatment and corticosteroid boluses due to the life-threatening situation (cardiopulmonary decompensation due to constrictive pericarditis, **Figure S1C-F**), anakinra was restarted three weeks after discontinuation. After stabilization, a successful pericardiectomy was performed and the patient, in August 2021, was able to undergo HSCT of a haploidentical sibling without major complications. Currently, the patient is alive and in remission, with no clinical signs of autoinflammation, normal monocytes count in PB, and complete chimera.

Anakinra treatment attenuates NLRP3 inflammasome activity

Since PBMCs from the index patient constitutively released IL-1β before anakinra treatment (**Figure 1B**), we aimed to find out whether this release was dependent on inflammasome activation. We cultured PBMCs from the index patient obtained just before anakinra administration and unstimulated or stimulated with LPS (lipopolysaccharide), LPS+ATP (adenosine triphosphate) for the NLRP3 inflammasome, or LPS+TcdB (*Clostridium difficile* toxin B) for the Pyrin inflammasome. In PBMCs from the index patient, the treatment with the NLRP3 inflammasome-specific blocker, MCC950, decreased IL-1β release in all conditions, except under stimulation of Pyrin inflammasome (LPS+TcdB) (**Figure 2A**). In contrast to healthy controls, in PBMCs from the index patient we did not observe increased IL-1β release with the LPS+ATP combination versus with LPS alone but did upon activation of the Pyrin inflammasome with LPS+TcdB (**Figure 2A**), suggesting maximal constitutive activation of NLRP3.

We next analyzed the presence of an ASC oligomer or speck in monocytes as a direct readout of active inflammasome formation by flow cytometry[24,25]. Surprisingly, our findings revealed that most monocytes from the pre-anakinra sample from the index patient presented ASC speck under resting conditions, and stimulation of the NLRP3 or Pyrin inflammasomes was not able to further induce changes (**Figure 2B**). As expected, in healthy donors, ASC oligomerization occurred only after NLRP3 inflammasome activation with LPS+ATP or Pyrin inflammasome activation with LPS+TcdB (**Figure 2B**). For representative assays see **Figure S2A-D**. In the index patient samples, application of MCC950 after priming with LPS, and before ATP or TcdB, was not able to reduce the percentage of monocytes with speck of ASC (**Figure 2B**), consistent with the fact that ASC oligomerization is an irreversible final step in inflammasome activation and, in this case, had already been induced before activation of NLRP3 or Pyrin by ATP

or TcdB, respectively. This could also explain the small release of IL-1β after NLRP3 or Pyrin activation compared with healthy donors (**Figure 2A**).

Importantly, after the first administration of anakinra, the percentage of basal ASC-specking monocytes of the index patient decreased and remained low at two time points examined during that treatment (**Figure 2C**), while the patient was clinically stable **(Figure 1C)**. Coinciding with new episodes of autoinflammation and discontinuation of anakinra, the percentage of ASC-specking monocytes increased, and decreased again after reintroduction of anakinra (**Figure 2C**). Furthermore, this therapy also favored the reduction of monocytes with ASC speck when the NLRP3 inflammasome was activated, *ex vivo,* by LPS+ATP (**Figure 2D**). In contrast, the percentage of monocytes with ASC speck formation after activation of the Pyrin inflammasome remained above 60% before and after anakinra treatment (**Figure 2D**). Accordingly, during such treatment, IL-1β and IL-18 release was not induced after *ex vivo* PBMCs stimulation with LPS or LPS+ATP, but was provoked when the Pyrin inflammasome was activated by LPS+TcdB (**Figure 2E, 2F**). During anakinra treatment, PBMCs from the index patient also showed increased tumor necrosis factor alpha (TNF-α) and IL-6 levels after stimulation with LPS, but this increase was less than the observed in PBMCs from healthy controls (**Figure S2E**). Altogether, these data suggest that blockade of the IL-1 pathway with anakinra can dampen the basal activation of the NLRP3 inflammasome, but not the activation of the Pyrin inflammasome.

Since it is known that inflammasome activation can lead to the release of ASC specks through pyroptosis[11,12], we next measured ASC in the patient's plasma. We found that the ASC plasma levels decreased after anakinra and during periods of clinical improvement under this therapy (**Figure 2G**). The elevation of ASC in the plasma before anakinra treatment and after anakinra withdrawn (**Figure 2G**) correlates with the increase of

monocytes with ASC speck in basal conditions (**Figure 2C**), suggesting that during periods of high ASC-specking monocytes, pyroptosis could be occurring *in vivo* in the patient and releasing ASC.

Accordingly, after treatment with anakinra, the levels of pro- and anti-inflammatory cytokines of the IL-1 family (IL-1α, IL-1β, IL-18, IL-18 binding protein [IL-18BP]) also decreased in the patient's plasma, whereas, in accordance with the mechanism of action of this agent, plasma levels of the IL-1 receptor antagonist (IL-1RA) increased (**Figure 2H**). Taken together, these data support that *in vivo* blockade of IL-1 signaling with anakinra in CMML *KRAS*^{mut} patients can reduce NLRP3 inflammasome overactivation and its deleterious inflammatory outcomes.

Clinical-biological characteristics of the cohort of CMML and MDS/MPN *KRAS*^{mut} patients

Based on the findings found in the index patient, we wondered whether other patients with CMML or MDS/MPN and *KRAS*^{mut} would have similar biological characteristics. To address this hypothesis, we sought the collaboration of participants from the Spanish Group of Molecular Biology in Hematology (GBMH). We retrospectively identified 19 patients. Patients' clinical-biological characteristics are summarized in **Table S1** and **Table S2**. According to WHO criteria, *KRAS*^{mut} patients were diagnosed with unclassifiable MDS/MPN (n=1), and CMML (n=18), 55.6% (10/18) MP subtype[1,2].

Cytogenetic study (CG) was available in 18 of the 19 patients, 3 of them (16.7%) (#4, 17 and 18) belonged to the intermediate/high CG risk-group[7]. Regarding molecular studies, we found 20 *KRAS* mutations in the 19 patients, the majority (19/20) in exon 2, with p.G12D being the most frequent. One patient (#15) harbored 2 mutations: p.G60D (exon

3) and p.G12R (exon 2). Interestingly, 5 patients (26.3%) had mutations in other genes of the RAS pathway, specifically, in *NRAS* (n=7). Moreover, 12 of 19 patients (63.2%) had mutations in other myeloid genes, being *TET2*, *SRSF2* and *ASXL1* the most frequent.

Prior to the diagnosis, or during follow-up, 10 of the 19 patients had autoinflammation and/or autoimmunity (**Table S1**). The most frequent were adenitis (5/19), including a Rosai-Dorfmann disease (#11); thyroid diseases (#11, 12, 19), and pneumonitis, pleuropericarditis and cellulitis (#1, 2). Three patients suffered more than one episode of autoinflammation (#1, 2, 11), with a median time between the onset of autoinflammatory episodes and the diagnosis of CMML of 5 years. Positive autoantibodies were detected in 2 of the 7 patients (#3, 4) for whom this information was available.

While 7 of the patients remain under observation, 12 received some form of hematological treatment; and 4 underwent allogeneic HSCT (#1, 5, 8, 18). With a median follow-up of 20 months, 42.1% of patients (8/19) had died.

NLRP3 inflammasome is activated in CMML *KRAS*^{mut} patients

For the inflammasome studies, fresh samples from treatment-free patients were required. We were able to collect and analyze fresh PB samples from five patients in the CMML *KRAS*^{mut} cohort (**Table S1,** #1, #3, #9, #11, #14) and from four CMML *KRAS*^{wt} patients (**Table S3,** #20, #21, #28, #29).

Similar to the index case, all CMML *KRAS*^{mut} patients had a significantly increased percentage of ASC-specking monocytes under resting and LPS priming conditions compared to healthy individuals and CMML *KRAS*^{wt} patients (**Figure 3A**). In CMML *KRAS*^{mut} patients, stimulation of the NLRP3 inflammasome was not able to increase the percentage of monocytes with ASC oligomers, suggesting that monocytes that could

respond to NLRP3 activation were already activated; whereas Pyrin inflammasome activation was able to increase the basal high percentage of ASC-specking monocytes, suggesting that there are some monocytes that were able to further activate Pyrin, but not, NLRP3 inflammasome. In healthy donors and *KRAS*^{wt} patients, by contrast, ASC oligomerization occurred only after activation of the NLRP3 or Pyrin inflammasome with LPS+ATP or LPS+TcdB, respectively (**Figure 3A**). Basal and induced IL-1β release with LPS and LPS+ATP in *KRAS*^{mut} patients was reduced by blocking the NLRP3 inflammasome with MCC950 (**Figure 3B**). Consistent with its specificity on the NLRP3 inflammasome, MCC950 was not able to significantly reduce IL-1β or ASC levels after activation of the Pyrin inflammasome with LPS+TcdB (**Figure 3B, 3C**). Except for the Pyrin inflammasome, the percentage of ASC-specking monocytes tended to decrease with MCC950, and this decrease was statistically significant when the NLRP3 inflammasome was activated (**Figure 3C**). However, after MCC950 treatment over 30% of monocytes remained with ASC speck (**Figure 3C**), in agreement with recent data demonstrating that this agent is effective on the inactive NLRP3 structure and is probably not able to affect the irreversible NLRP3-ASC oligomer already formed[26]. As expected, in our cohort of CMML patients an increase percentage of circulating monocytes was found (**Figure S2F**), being in agreement with the increased myeloid colony formation and the defective apoptosis of monocytes in these patients[27,28]. When analyzing the gene expression omnibus GSE135902 database[29], we found that in CMML patients with *RAS*^{mut} there were less expression of gasdermin D gene, despite elevation of *NLRP3* and *IL1B* gene expression (**Figure S2G**). Also, extracellular LDH levels normalized to the percentage of monocytes did not increase in unstimulated cultured PBMCs from CMML patients with *KRAS*^{mut} (**Figure 3D**). This suggests that despite a basal activation of the inflammasome in CMML *KRAS*^{mut} monocytes, there could be a defective pyroptosis and

a potential hyperactive state of the monocytes, where active inflammasome would result in IL-1β release from living cells[30-32]. Regardless the viability of *in vitro* cultured CMML *KRAS*^{mut} monocytes, in CMML patient's plasma an increase in high mobility group box 1 (HMGB1), and especially in the soluble form of the P2X purinoceptor 7 receptor (P2X7) in patients with a *KRAS* mutation was observed (**Figure 3E**), suggesting that *in vivo* pyroptosis or other type of cell death could be occurring in patients with CMML *KRAS*^{mut}.

Next, we evaluate the status of NLRP3 inflammasome pathway coding genes in the index CMML *KRAS*^{mut} patient by whole-exome sequencing. The presence of pathogenic variants in any of the inflammasome-associated genes were discarded (**Table S4**).

Circulating levels of inflammatory cytokines in CMML *KRAS*^{mut} patients

Since an increase of different markers associated with pyroptosis was observed in the plasma of CMML *KRAS*^{mut} patients, we next compared whether the circulating profile of inflammatory cytokines was also different compared to controls. Our data showed that, compared to healthy controls, the CMML *KRAS*^{wt} patients only showed statistical differences in IL-6 (**Figure 4A, 4B**). In contrast, CMML *KRAS*^{mut} patients displayed significantly higher levels of inflammasome- and nuclear factor kappa B (NF-κB) associated cytokines (IL-1α, IL-1RA, IL-12 p40 and IL-18) and lower levels of MCP-1 than healthy controls and CMML *KRAS*^{wt} patients (**Figure 4A, 4B**). IL-18 was the cytokine with the largest differences: 28.4 ± 7.9 vs. 1287.0 ± 762.8 pg/ml in CMML *KRAS*^{wt} and *KRAS*^{mut} patients, respectively ($p < 0.01$) (**Table S5**).

As we expected, our results demonstrate that CMML *KRAS*^{mut} patients had significantly higher levels of IL-1α, IL-1β, IL-12 p40 and IL-12 p70, but lower levels of IL-6 and

MCP-1, than sepsis patients (as disease controls with acute inflammation) (**Figure 4A** and **Table S5**). Overall, in agreement with the activation of the NLRP3 inflammasome, CMML *KRAS*^{mut} patients present an increase of circulating inflammasome-dependent cytokines.

Moreover, genetic and/or biological parameters other than *KRAS* mutation that could influence the higher cytokine levels observed in CMML *KRAS*^{mut} patients were investigated. Thus, in the full CMML patient cohort (n=17), we observed that none of elevated cytokines in CMML *KRAS*^{mut} (vs *KRAS*^{wt}) patients (IL-1α, IL-1RA, IL-12 p40 and p70, and IL-18) was significantly different when comparing patients according to the presence or absence of the most frequently found mutations (*TET2*, *SRSF2*, or *ASXL1*), or CMML variant (MP vs MD) (**Table S6**).

DISCUSSION

RAS mutations are found in 20-30% of all human malignancies, such as CMML (7-22%)[33,34] and juvenile myelomonocytic leukemia (JMML) (20-25%)[1,2,34], and mainly affect codons 12 and 13 of exon 2. Mutations in key residues in exon 2 or exon 3 [positions 10-14 (P-loop region) and 58-72 (Switch-II region)] affect the GTP-binding site, preventing the conversion of the active RAS-GTP into inactive RAS-GDP[35,36], leading to the continued activation of its downstream targets MEK1/2 and ERK1/2[37], promoting cell proliferation and survival. However, since the RAS/RAF/MEK/ERK cascade couples cell surface receptor signals to transcription factors in both malignant and non-malignant immune cells[38], recent studies have attempted to investigate whether myeloid clonal proliferation may be mediated not only by a direct oncogenic stimulus, but also by inflammatory mechanisms.

The NLRP3 inflammasome has been implicated in different diseases, including MDS[16,18,39,40], although this evidence comes mainly from models of NLRP3- or caspase-1-deficient mice or treating animals with experimental NLRP3 blockers[16,41]. Few studies address NLRP3 in the context of human disease, mainly due to the complexity of the signaling pathway, involving an NLRP3 oligomerization step to recruit ASC and activate caspase-1[42,43]. Basal ASC oligomerization has been found in MDS bone marrow (BM) progenitor cells[39,40], but has not been found, so far, in unstimulated human circulating monocytes of any human disease. Here, we describe that in *KRAS*^{mut} CMML there is an increased percentage of circulating monocytes with ASC oligomers in PB under basal conditions. This result has not been even described for cryopyrin-associated periodic syndrome (CAPS) patients, who present gain-of-function mutations in NLRP3. Monocytes of CAPS patients increase the percentage of ASC-specking monocytes after

LPS stimulation, avoiding the second signal of NLRP3 activation[44–46]. The NLRP3 inflammasome is a cellular irreversible mechanism once ASC oligomerize, and since CMML monocytes already present ASC oligomers at basal level, NLRP3 inhibition will not be able to block these already formed inflammasomes. The identification of the inflammasome sensor behind the ASC oligomer found in monocytes from CMML *KRAS*^{mut} patients is a challenging question; upon culturing blood with the specific NLRP3 blocker MCC950[26,46–48], the percentage of monocytes with ASC oligomers slightly decreases, while IL-1β release is significantly affected. This, together with the fact that no increased IL-1β release was achieved after the canonical NLRP3 activation with LPS+ATP, supports the idea that mutations in *KRAS* might be inducing NLRP3 activation, as recently reported in a mouse model and in human leukemia cells with a *KRAS*^{G12D} mutation[9].

The basal activation of the inflammasome in CMML *KRAS*^{mut} patients was not associated to a pyroptosis of the monocytes, as they could be cultured and were not releasing LDH, suggesting that IL-1β could be released from living hyperactive cells, a state of the cell found in macrophages and dendritic cells after certain inflammasome stimulation conditions[30-32]. Defective pyroptosis of monocytes from CMML *KRAS*^{mut} patients would support the high viability of the cells while producing IL-1β and could represent another mechanism of cell survival together the defective apoptosis found in CMML monocytes[28]. However, in the patients' plasma we found an increase of cell-death markers such as HMGB1, ASC and the P2X7 receptor. While, we have recently found the latter in the supernatants of human PBMCs after inflammasome activation[49], HMGB1 and ASC alarmins have been reported to be released from dying cells, including but not exclusively from pyroptotic cells[11,12,50,51]. ASC has been found elevated in the serum of patients with autoinflammatory diseases, in HIV-infected persons, as well as in the bronchoalveolar

lavage of individuals with chronic obstructive pulmonary disease[11,12,50]. In myeloid neoplasia, Basiorka *et al*. showed increased ASC oligomers in plasma of MDS patients, especially in low-risk disease[40], compared to patients with other hematological cancers, and suggested that ASC specks in plasma could be a biomarker for the differential diagnosis of MDS versus other hematological cancers, including CMML[40]. Our results, however, would not support their use as a surrogate marker for MDS-specific pyroptosis. Consistent with basal NLRP3 inflammasome activation, CMML *KRAS*^{mut} patients showed higher levels of inflammasome-associated cytokines (IL-1α, IL-1β and IL-18), compared to CMML *KRAS*^{wt} patients. Also, higher levels of NF-κB pathway-associated cytokines (IL-6, IL-8 and IL-12), and M-CSF, were evidenced compared to healthy controls. Our results agree with data analyzing other *KRAS* mutated cancers, in which an increase in some of these cytokines has been described[52]. Specifically, in CMML, Niyongere *et al*. found that mutations in genes involved in signaling pathways (*JAK2, NRAS, KRAS, CBL*) had higher plasma levels of IL-12 p40, and IL-1RA[53].

Our findings also provide insights into possible novel therapeutic strategies in CMML *KRAS*^{mut} patients, who have a poorer response to conventional treatments[22]. Extracellular oligomers of ASC propagate inflammasome-dependent inflammation[11,12] and could be pharmacologically disaggregated by a, very recently developed, nanobody that has been used in animal models of inflammation[13]. Pharmacological inhibition of vitro NLRP3 suppressed pyroptosis and restored effective hematopoiesis *in vitro* and in a mouse model of MDS[39]. Our study supports the notion that CMML *KRAS*^{mut} patients could be candidates for therapies directed not only against NLRP3, but also against extracellular ASC oligomers. Although some NLRP3 blockers are entering early clinical trials, they are not yet approved for clinical use, and the only treatments available for patients with inflammasomopathies are IL-1[54] blockers: anakinra and canakinumab. Here we show that

treatment of a CMML *KRAS*^{G12D} mutated patient with anakinra not only improved clinical status and monocytic proliferation, but also blocked NLRP3 inflammasome activation in *ex vivo* experiments. This suggests the interesting hypothesis that proliferation of malignant monocyte clones might depend on IL-1 signaling and that its blockade influences NLRP3 activation, with this cytokine probably being a positive regulator for NLRP3 priming and activation. In fact, it has been recently shown that IL-1 contributes to malignant myeloproliferation[55].

Since mutations in *KRAS/NRAS* are not unique to patients with CMML, our findings could be extended to other myeloid diseases such as juvenile CMML, MDS, and AML with mutations in the RAS pathway. Indeed, Basiorka *et al*. found that NLRP3 inflammasome activation was responsible for many of the hallmarks of MDS, such as macrocytosis and ineffective hematopoiesis[39]. On the other hand, these authors found that mutations in other myeloid genes, beyond *RAS,* can also induce NLRP3 inflammasome activation (*U2AF1, SF3B1, SRSF2, ASXL1* and *TET2*)[39]. In our cohort of CMML patients in whom inflammasome studies were performed, 4 of the 5 *KRAS*^{mut} patients had only *KRAS* mutation. In contrast, each of the 4 CMML *KRAS*^{wt} patients carried a different mutational profile; and all of them presented mutations in splicing genes and epigenetic modifiers (*TET2, ASXL1* and/or *SRSF2),* which occur in up 80% of patients with CMML[1], being, therefore, a representative sample of CMML patients. Given that genetically the main difference between the two cohorts of patients is the presence of mutations in *KRAS*, the high basal inflammasome activation that we observed in CMML *KRAS*^{mut} patients can only be explained by aberrant KRAS signaling. However, due to the size of our cohort, we cannot rule out that mutations in myeloid genes other than *KRAS* may also influence on inflammasome activation. In fact, previous studies have shown that the proportion of pyroptotic erythroid progenitors in BM samples from MDS patients increases with the

complexity of the mutations and the allelic burden[39]. In line with these authors, the mean *KRAS*^{mut} allele burden of the patients in our series in whom NLRP3 inflammasome study could be performed was higher than 40%. Among them, those with an allelic burden close to 50% were associated with repetitive and severe episodes of autoinflammation. This is not surprising, since the RAS/RAF/MEK/ERK pathway is also involved in the control of B-cell tolerance and autoantibody production[56,57]. Consistent with our findings, very recently, Andina *et al*, have shown that NLRP3 dysregulation in CMML positively correlated with disease severity[58].

Taken together, our study demonstrates using functional assays that in a cohort of CMML *KRAS*^{mut} patients there is a basal activation of the NLRP3 inflammasome and a specific inflammatory cytokine signature. At present, the IL-1R blocker (anakinra) may be a therapeutic option to be considered to improve the clinical status, control monocytic proliferation and NLRP3 inflammasome activation. In the future, inflammasome blockade with different therapies may offer new opportunities for patients with myeloid neoplasms and *RAS* mutations.

Limitations of the study

The principal limitation of the study is the small sample size of cohort of primary CMML samples. According to that: i) only a case report of a patient with KRAS-mutated CMML successfully quelled by Anakinra treatment with subsequent bridging to allograft is presented; and ii) although our data suggests that only KRASmut monocytes have constitutively active the NLRP3 inflammasome; the cohort of KRASWT patients is too small and we cannot rule out that mutations in myeloid genes other than KRAS may have a similar effect on the NLRP3 inflammasome. Therefore, it would be interesting to (1) study additional samples in the experimental studies (both from KRASmut and KRASWT

CMML patients); (2) to expand the subgroup comparisons to MAPK-mutated cases, cases with mutations in other RAS pathway genes (NRAS, CBL and PTPN11), or signaling-related genes beyond RAS pathway; and (3) finally, to observe the impact of the newly available specific inhibitors of KRAS on in vitro experiments to activate the NLRP3 inflammasome.

STAR METHODS

Detailed methods are provided in the online version of this paper and include the following:

- KEY RESOURCES TABLE
- RESOURCE AVAILABILITY
    - Lead contact
    - Materials availability
    - Data and code availability
- EXPERIMENTAL MODEL AND STUDY PARTICIPANT DETAILS
    - Patients and cohorts
    - Human clinical samples
- METHODS DETAILS
    - Cells and treatments
    - Evaluation of monocytes with ASC by flow cytometry
    - Lactate dehydrogenase assay
    - Cytokine evaluation
    - Sequencing samples
    - Whole exome sequencing
- QUANTIFICATION AND STADISTICAL ANALYSIS

RESOURCE AVAILABILITY

Lead contact

Further information and requests for resources and reagents should be directed to and will be fulfilled by the lead contact Pablo Pelegrín (pablo.pelegrin@imib.es)

Materials availability

This study did not generate new unique reagents.

Data and code availability

- The raw sequence data used for analysis is available in NCBI under the Sequence Read Archive (SRA: www.ncbi.nlm.nih.gov/sra) with BioProject No. PRJNA1032543 (see Key Resources table). The patient level data reported in this study cannot be deposited in a public repository because of limitations associated with the informed consent. All other original data generated during this study has been deposited at Zenodo (zenodo.org) and is publicly available as of the date of publication. DOI is listed in the Key Resources table.
- This paper does not report original code.
- Any additional information required to reanalyze the data reported in this paper is available from the lead contact upon request.

EXPERIMENTAL MODEL AND STUDY PARTICIPANT DETAILS

Patients and cohorts

The clinical-biological characteristics of 19 patients diagnosed with MDS/MPN with mutations in exon 2 or exon 3 of *KRAS* (*KRAS*^{mut}) were collected from 7 Spanish highly-specialized hospitals in hematologic molecular diagnosis. Plasma samples at diagnosis from 9 out of the 19 patients were included for this study. Since most of the patients had died or were under hematological treatment, fresh (PB) peripheral blood was available in only 5 patients (**Table S1**) who, at the time of the study, were alive and untreated. From one of them, index case (**Table S1,** patient #1), PB samples were collected at different times. The study also included CMML patients (n=10) without mutations in exon 2 or 3 of *KRAS* (*KRAS*^{wt}), in whom plasma samples (n=8), and fresh PB (n=4) were collected (**Table S3**). We used, as controls, healthy individuals (n=9), matched in age and sex with the *KRAS*^{mut} patients, and patients with sepsis (n=5). This study was approved by the Clinical Research Ethics Committee of the Hospital Universitario Morales-Meseguer in Murcia, Spain (reference no. 07/19).

Human clinical samples

CMML patients' samples were collected from the following hospitals: Hospital General Universitario Morales-Meseguer (Murcia), Hospital Universitario y Politécnico La Fe (Valencia); Hospital Clínico Universitario de Valencia (Valencia), Complejo Universitario de Salamanca (Salamanca), Hospital Universitario 12 de octubre (Madrid), Hospital del Mar, and ICO-Hospital Germans Trias i Pujol (both located in Barcelona). Samples from healthy individuals and patients with sepsis, used as controls, were stored in the Biobank Network of the Region of Murcia [PT13/0010/0018 integrated in the National Biobank Network (B.000859)].

Clinical and demographic characteristics of patients analyzed in this study are provided in **Table S1**, **Table S2** and **Table S3**. All patients gave informed consent and studies were

approved by their respective ethical review committees. Raw sequencing data from patient samples from Hospital General Universitario Morales-Meseguer have been deposited at Sequence Read Archive (SRA) with BioProject No. PRJNA1032543.

METHODS DETAILS

Cells and treatments

Whole PB samples were cultured with RPMI 1640 medium (Lonza) containing 10% fetal calf serum (FCS, Cytiva) and 2 mM GlutaMax (Thermo Fisher Scientific). In some experiments, PB mononuclear cells (PBMC) were collected using Ficoll Histopaque-1077 (#10771, Sigma-Aldrich) and 500.000 cells were cultured in 24 well cell culture plate in 500µl of Opti-MEM Reduced Serum Media (#51985-026, Gibco). PB or PBMCs were treated with 1.6 µg/ml lipopolysaccharide (LPS) for 2 h at 37°C, and subsequently stimulated with 3 mM adenosine 5'-triphosphate (ATP) for 30 min (to trigger NLRP3 inflammasome activation) or 1 µg/ml Clostridium difficile toxin B (TcdB) for 1h (to trigger Pyrin inflammasome activation). In some cases, 10 µM MCC950 was added 10 min before ATP or TcdB and maintained during stimulation.

Evaluation of monocytes with ASC by flow cytometry

For the evaluation of monocytes with ASC by flow cytometry, PB treatment with ATP was for 15 min and TcdB for 30 min. After treatment erythrocytes were lysed under mild hypotonic conditions while preserving and fixing leukocytes with FACS lysing/fixing solution (#349202, BD Biosciences). Monocytes were stained and gated with fluorescein (FITC)-conjugated mouse anti-CD14 monoclonal antibody (clone M5E2; catalog #557153; BD Biosciences, 1:10). The detection of ASC specks in monocytes was done

by Time-of-Flight Inflammasome evaluation technique, as we have recently described[24,25] using phycoerythrin (PE)-conjugated mouse anti-ASC monoclonal antibody (HASC-71 clone; #653903; BioLegend, 1:500) and the FACS-Canto flow cytometer (BD Biosciences). Data was analyzed with the FCS Express Software (De Novo Software). For gating strategy and representative results see **Figure S2A-D**.

Lactate dehydrogenase assay

To measure cell death, lactate dehydrogenase (LDH) present in cell-free supernatants was detected using the Cytotoxicity Detection kit (Roche) according to manufacturer instructions, the reaction was read in a Synergy Mx (BioTek) plate reader at 492 nm and corrected at 620 nm.

Cytokine evaluation

Plasma or cell-free supernatants from fresh EDTA-anticoagulated PB samples from CMML patients and controls were used to quantify the concentration of human IL-1β (#BMS224INST, Invitrogen), human IL-18 (#7620, MBL), human IL-18BP (#EHIL18BP, Invitrogen), human TNF-α (#DTA00D, R&D Systems), human IL-6 (#D6050, R&D Systems), human ASC (#CSB-EL019114HU, Cusabio), human soluble P2X7 receptor (#CSB-EL017325HU, Cusabio), and human HMGB1 (#ARG81185, Arigo Biolaboratories) by ELISA following the manufacturer's instructions. Results were read on a Synergy Mx plate reader (BioTek) at 450 nm and corrected at 540 nm and 620 nm. Plasma levels of 15 inflammatory cytokines associated with NLRP3-inflammasome, NF-κB and other inflammatory pathways [IL-1α, IL-1β, IL-1RA, IL-12 (p40 and p70), IL-18, IL-6, IL-8, TNF-α, IL-15, MCP-1/CCL2, M-CSF, GM-CSF, IL-2 and IL-10] were

measured using a custom MILLIPLEX® kit (#HCYTA-60K, Millipore). A MAGPIX® system (Luminex), using xPONENT® software, was used for analysis, and the cytokines concentrations were obtained using MilliplexAnalyst v.5.2 Flex software (VigeneTech). GM-CSF, IL-2 and IL-10 were not analyzed as they were not detected in most samples.

Sequencing analysis

High-throughput sequencing by gene panel (HTS) was performed on diagnostic samples from patients included as CMML (n=28) or MDS/MPN (n=1). The HTS panel included at least the following 22 genes related to myeloid disorders (ASXL1, CALR, CBL, CSF3R, DNMT3A, ETV6, EZH2, IDH1, IDH2, JAK2, KIT, KRAS, MPL, NRAS, RUNX1, SETBP1, SF3B1, SRSF2, TET2, TP53, U2AF1 and ZRSR2), BioProject PRJNA1032543. Briefly, DNA was extracted from PB or bone marrow (BM) samples and, once the library was ready, amplified on Illumina platforms (MiSeq and NextSeq 500). Results were analyzed using the SOPHiA DDM platform with its proprietary pipeline or in-house pipelines from Galaxy platform tools (FastQC for quality control, BWA/Bowtie2 for genome alignment and SAMtools for variant calling). Only pathogenic variants with a variant allele frequency (VAF) greater than 2% or more than 10 mutated reads were reported.

Whole exome sequencing

Whole-exome sequencing was performed by using NovaSeq 6000 (Illumina). Libraries to be sequenced were generated using WES SureSelectXT kit (Agilent Technologies) and the protocol “SureSelectXT Target Enrichment System for Illumina Version B.2, April 2015”. The reads obtained were paired-end (2x150bp), with an average depth per

nucleotide of 100 reads, 150 million reads per sample and Phred Quality Score 30 (Q30) >95%, generating a file of between 10-15 GB per sample, in a FASTQ format (BioProject PRJNA1032543). Bioinformatics analysis was performed using validated tools from BaseSpace (Illumina). Initial prioritization of both somatic and germline variants was performed using its proprietary pipeline (DRAGEN Somatic or DRAGEN Germline, respectively), and CLC Genomics Workbench (Qiagen) for variant calling, eliminating intronic, synonymous and those with a minor allelic variant greater than or equal to 1%. The final prioritization of germline variants was performed according to the criteria of the American College of Medical Genetics / Association of Molecular Pathologists (ACMG / AMP) and somatic variants were defined as recurrently mutated variants that had been reported by more than one author in the main databases (COSMIC, TP53 Database, ClinVar). Finally, for the index patient, we filtered for genes known to be involved in inflammasome-related diseases (**Table S4**).

QUANTIFICATION AND STATISTICAL ANALYSIS

Statistical analyses were performed using GraphPad Prism version 9 (GraphPad Software Inc.). Continuous variables were presented as mean ± SEM or median (interquartile range, IQR), as appropriate, and categorical variables were presented as percentages. Comparisons of categorical variables between groups were performed using the χ^2 test for tables, while continuous variables were compared using the two-tailed Student's t test or the Mann-Whitney U test, as appropriate. Normality of values was determined with the D'Agostino and Pearson omnibus K2 normality test. For comparisons between two groups do not following normality distribution, the two-tailed Mann-Whitney U test was applied, setting the significance level at $p<0.05$. For dataset GSE135902 gene expression

comparison, the Wilcoxon signed rank tests with Benjamini–Hochberg correction was used.

Acknowledgments

We are particularly grateful for the generous contribution of the patients and healthy donors. We would like to thank Lourdes Martinez and Juana M. Plasencia (Radiology Department) and Mª José López Poveda (Pathology Department) of the Hospital Morales-Meseguer for their help in the selection of the images; and MC Baños and AI Gomez (IMIB) for technical support, and all the members of Dr. Pelegrin's laboratory for comments and suggestions. We are indebted to GBMH, Marta Martín (IBSAL, Salamanca), Mar Tormo (Clinic University Hospital, Valencia) and Ana Garrido (Sant Pau Hospital, Barcelona) for contributing to the execution of the present study. We also thank the collaboration of Biobank Network of the Region of Murcia, BIOBANC-MUR, registered on the *Registro Nacional de Biobancos* with registration number B.0000859. BIOBANC-MUR is supported by the *Instituto de Salud Carlos III* (grant PT20/00109), by *Instituto Murciano de Investigación Biosanitaria* and by *Consejería de Salud de la Comunidad Autónoma de la Región de Murcia*.

Authors' Contributions

LH-N, HM-B, EJC-Z, MLM and RT-M: experimental execution; LM-A, CG-P and ES-E: sample collection; LH-N, EJC-Z, ES-E, RT-M, THC-L FF-M and PP: data analysis; FF-M and PP: conceived the experiments; LH-N and EJC-Z prepared the figures. All other authors contributed to patient data and/or material for analysis. FF-M and PP: conceived the experiments, wrote the paper, provided funding and overall supervision of the study. All authors approved the final version of the manuscript.

Declaration of interests

PP is consultant of Viva In Vitro Diagnostics SL. PP, HM-B and CG-P are inventors on patent PCT/EP2020/056729. LH-N, LM-A, HM-B, CG-P and PP are co-founders of Viva In Vitro Diagnostics SL but declare that the research was conducted in the absence of any commercial or financial relationships that could be construed as a potential conflict of interest. The other authors declare no competing interests.

REFERENCES

1. Arber, D. A., Orazi, A., Hasserjian, R, P., et al. (2022). International Consensus Classification of Myeloid Neoplasms and Acute Leukemias: integrating morphologic, clinical, and genomic data. Blood 140, 1200-1228. doi:10.1182/blood.2022015850

2. Khoury, J. D., Solary, E., Abla, O., et al. (2022). The 5th edition of the World Health Organization Classification of Haematolymphoid Tumours: Myeloid and Histiocytic/Dendritic Neoplasms. Leukemia 36, 1703-1719. doi:10.1038/s41375-022-01613-1

3. Reiter, A., Invernizzi, R., Cross, N. C. P., Cazzola, M. (2009). Molecular basis of myelodysplastic/myeloproliferative neoplasms. Haematologica 94, 1634-1638. doi:10.3324/haematol.2009.014001

4. Kohlmann, A., Grossmann, V., Klein, H. U., et al. (2010). Next-Generation Sequencing Technology Reveals a Characteristic Pattern of Molecular Mutations in 72.8% of Chronic Myelomonocytic Leukemia by Detecting Frequent Alterations in *TET2* , *CBL* , *RAS* , and *RUNX1*. Journal of Clinical Oncology 28, 3858-3865. doi:10.1200/JCO.2009.27.1361

5. Carr, R. M., Vorobyev, D., Lasho, T., et al. (2021). RAS mutations drive proliferative chronic myelomonocytic leukemia via a KMT2A-PLK1 axis. Nat. Commun. 12, 2901. doi:10.1038/s41467-021-23186-w

6. Itzykson, R., Kosmider, O., Renneville, A., et al. (2013). Prognostic Score Including Gene Mutations in Chronic Myelomonocytic Leukemia. Journal of Clinical Oncology31, 2428-2436. doi:10.1200/JCO.2012.47.3314

7. Such, E., Germing, U., Malcovati, L., et al. (2013). Development and validation of a prognostic scoring system for patients with chronic myelomonocytic leukemia. Blood121, 3005-3015. Doi:10.1182/blood-2012-08-452938

8. McCubrey, J. A., Steelman, L. S., Chappell, W. H., et al. (2007). Roles of the Raf/MEK/ERK pathway in cell growth, malignant transformation and drug resistance. Biochimica et Biophysica Acta (BBA) - Molecular Cell Research 1773, 1263-1284. doi:10.1016/j.bbamcr.2006.10.001

9. Hamarsheh, S., Osswald, L., Saller, B. S., et al. (2020). Oncogenic KrasG12D causes myeloproliferation via NLRP3 inflammasome activation. Nat. Commun. 11, 1659. doi:10.1038/s41467-020-15497-1

10. Broz, P., Pelegrín, P., Shao, F. (2020). The gasdermins, a protein family executing cell death and inflammation. Nat. Rev. Immunol. 20, 143-157. doi:10.1038/s41577-019-0228-2

11. Baroja-Mazo, A., Martín-Sánchez, F., Gómez, A. I., et al. (2014). The NLRP3 inflammasome is released as a particulate danger signal that amplifies the inflammatory response. Nat. Immunol. 15, 738-748. doi:10.1038/ni.2919

12. Franklin, B. S., Bossaller, L., De Nardo, D., et al. (2014). The adaptor ASC has extracellular and “prionoid” activities that propagate inflammation. Nat. Immunol. 15, :727-737. doi:10.1038/ni.2913

13. Bertheloot, D., Wanderley, C. W., Schneider, A. H., et al. (2022). Nanobodies dismantle post-pyroptotic ASC specks and counteract inflammation *in vivo*. EMBO Mol. Med. 14, e15415. doi:10.15252/emmm.202115415

14. Groß, C. J., Mishra, R., Schneider, K. S., et al. (2016). K + Efflux-Independent NLRP3 Inflammasome Activation by Small Molecules Targeting Mitochondria. Immunity 45, 761-773. doi:10.1016/j.immuni.2016.08.010

15. Tapia-Abellán, A., Angosto-Bazarra, D., Alarcón-Vila, C., et al. (2021). Sensing low intracellular potassium by NLRP3 results in a stable open structure that promotes inflammasome activation. Sci. Adv. 7, 4468-4483. doi:10.1126/sciadv.abf4468

16. Coll, R. C., Schroder, K., Pelegrín, P. (2022). NLRP3 and pyroptosis blockers for treating inflammatory diseases. Trends Pharmacol. Sci. 43, 653-668. doi:10.1016/j.tips.2022.04.003

17. Comont, T., Treiner, E., Vergez, F. (2021). From Immune Dysregulations to Therapeutic Perspectives in Myelodysplastic Syndromes: A Review. Diagnostics 11, 1982. doi:10.3390/diagnostics11111982

18. Sallman, D. A., List, A. (2019). The central role of inflammatory signaling in the pathogenesis of myelodysplastic syndromes. Blood 133, 1039-1048. doi:10.1182/blood-2018-10-844654

19. Robin, M., de Wreede, L. C., Padron, E., et al. (2022). Role of allogeneic transplantation in chronic myelomonocytic leukemia: an international collaborative analysis. Blood 140, 1408-1418. doi:10.1182/blood.2021015173

20. de Witte, T., Bowen, D., Robin, M., et al. (2017). Allogeneic hematopoietic stem cell transplantation for MDS and CMML: recommendations from an international expert panel. Blood129, 1753-1762. doi:10.1182/blood-2016-06-724500

21. Patnaik, M. M., Tefferi, A. (2018). Chronic myelomonocytic leukemia: 2018 update on diagnosis, risk stratification and management. Am. J. Hematol. 93, 824-840. doi:10.1002/ajh.25104

22. Lasho, T., Patnaik, M. M. (2021). Novel therapeutic targets for chronic myelomonocytic leukemia. Best Pract. Res. Clin. Haematol. 34, 101244. doi:10.1016/j.beha.2021.101244

23. Zhao, L. P., Schell, B., Kim, R., et al. (2021). MDS-029: Prevalence of VEXAS Syndrome in MDS/CMML Patients with Systemic Inflammatory and Auto-Immune Disease. Clin Lymphoma Myeloma Leuk. 21, S337-S338. doi:10.1016/S2152-2650(21)01788-2

24. Sester, D. P., Thygesen, S. J., Sagulenko, V., et al. (2015). A Novel Flow Cytometric Method To Assess Inflammasome Formation. The Journal of Immunology 194, 455-462. doi:10.4049/jimmunol.1401110

25. Hurtado-Navarro, L., Baroja-Mazo, A., Martínez-Banaclocha, H., Pelegrín, P. (2022). Assessment of ASC Oligomerization by Flow Cytometry. In: Abdul-Sater, A.A. (eds) The Inflammasome. Methods in Molecular Biology1-9. doi:10.1007/978-1-0716-2144-8_1

26. Hochheiser, I. V., Pilsl, M., Hagelueken, G., et al. (2022). Structure of the NLRP3 decamer bound to the cytokine release inhibitor CRID3. Nature604, 184-189. doi:10.1038/s41586-022-04467-w

27. Geissler, K., Jäger, E., Barna, A., et al. (2016). Chronic myelomonocytic leukemia patients with RAS pathway mutations show high in vitro myeloid colony formation in the absence of exogenous growth factors. Leukemia30, 2280–2281. doi.org/10.1038/leu.2016.235

28. Sevin, M., Debeurme, F., Laplane, L., et al. (2021). Cytokine-like protein 1-induced survival of monocytes suggests a combined strategy targeting MCL1 and MAPK in CMML. Blood137, 3390–3402. doi.org/10.1182/blood.2020008729

29. Franzini, A., Pomicter, A. D., Yan, D., et al. (2019). The transcriptome of CMML monocytes is highly inflammatory and reflects leukemia-specific and age-related alterations. Blood advances 3, 2949–2961. doi.org/10.1182/bloodadvances.2019000585

30. Evavold, C. L., Ruan, J., Tan, Y., et al. (2018). The Pore-Forming Protein Gasdermin D Regulates Interleukin-1 Secretion from Living Macrophages. Immunity48, 35–44.e6. doi.org/10.1016/j.immuni.2017.11.013

31. Zanoni, I., Tan, Y., Di Gioia, M., et al. (2016). An endogenous caspase-11 ligand elicits interleukin-1 release from living dendritic cells. Science352, 1232-1236. Doi.org/10.1126/science.aaf3036

32. Lieberman, J., Wu, H., Kagan, J. C. (2019). Science Immunology 4, eaav1447. Doi.org/10.1126/sciimmunol.aav1447

33. Itzykson, R., Fenaux, P., Bowen, D., et al. (2018). Diagnosis and Treatment of Chronic Myelomonocytic Leukemias in Adults. Hemasphere2, e150. doi:10.1097/HS9.0000000000000150

34. Patnaik, M. M., Lasho, T. (2020). Evidence-Based Minireview: Myelodysplastic syndrome/myeloproliferative neoplasm overlap syndromes: a focused review. Hematology2020, 460-464. doi:10.1182/hematology.2020000163

35. Johnson, C. W., Reid, D., Parker, J. A., et al. (2017). The small GTPases K-Ras, N-Ras, and H-Ras have distinct biochemical properties determined by allosteric effects. Journal of Biological Chemistry 292, 12981-12993. doi:10.1074/jbc.M117.778886

36. Pantsar, T. (2020). The current understanding of KRAS protein structure and dynamics. Comput. Struct. Biotechnol. J. 18, 189-198. doi:10.1016/j.csbj.2019.12.004

37. Meynier, S., Rieux-Laucat, F. (2020). After 95 years, it's time to eRASe JMML. Blood Rev. 43, 100652. doi:10.1016/j.blre.2020.100652

38. Cobb, M. H., Goldsmith, E. J. (1995). How MAP Kinases Are Regulated. Journal of Biological Chemistry270, 14843-14846. doi:10.1074/jbc.270.25.14843

39. Basiorka, A. A., McGraw, K. L., Eksioglu, E. A., et al. (2016). The NLRP3 inflammasome functions as a driver of the myelodysplastic syndrome phenotype. Blood 128, 2960-2975. doi:10.1182/blood-2016-07-730556

40. Basiorka, A. A., McGraw, K. L., Abbas-Aghababazadeh, F., et al. (2018). Assessment of ASC specks as a putative biomarker of pyroptosis in myelodysplastic syndromes: an observational cohort study. Lancet Haematol. 5, e393-e402. doi:10.1016/S2352-3026(18)30109-1

41. Mangan, M. S. J., Olhava, E. J., Roush, W. R., Seidel, H. M., Glick, G. D., Latz, E. (2018). Targeting the NLRP3 inflammasome in inflammatory diseases. Nat. Rev. Drug Discov. 17, 588-606. doi:10.1038/nrd.2018.97

42. Schmidt, F. I., Lu, A., Chen, J. W., et al. (2016). A single domain antibody fragment that recognizes the adaptor ASC defines the role of ASC domains in inflammasome assembly. Journal of Experimental Medicine213, 771-790. doi:10.1084/jem.20151790

43. Lu, A., Li, Y., Schmidt, F. I., et al. (2016). Molecular basis of caspase-1 polymerization and its inhibition by a new capping mechanism. Nat. Struct. Mol. Biol. 23, 416-425. doi:10.1038/nsmb.3199

44. Mensa-Vilaro, A., Bosque, M. T., Magri, G., et al. (2016). Brief Report: Late-Onset Cryopyrin-Associated Periodic Syndrome Due to Myeloid-Restricted Somatic *NLRP3* Mosaicism. Arthritis & Rheumatology68, 3035-3041. doi:10.1002/art.39770

45. Weber, A. N. R., Tapia-Abellán, A., Liu, X., et al. (2022). Effective *ex vivo* inhibition of cryopyrin-associated periodic syndrome (CAPS)-associated mutant NLRP3 inflammasome by MCC950/CRID3. Rheumatology61, e299-e313. doi:10.1093/rheumatology/keac273

46. Tapia-Abellán, A., Angosto-Bazarra, D., Martínez-Banaclocha, H., et al. (2019). MCC950 closes the active conformation of NLRP3 to an inactive state. Nat. Chem. Biol. 15, 560-564. doi:10.1038/s41589-019-0278-6

47. Coll, R. C., Robertson, A. A. B., Chae, J. J., et al. (2015). A small-molecule inhibitor of the NLRP3 inflammasome for the treatment of inflammatory diseases. Nat. Med. 21, 248-255. doi:10.1038/nm.3806

48. Coll, R. C., Hill, J. R., Day, C. J., et al. (2019). MCC950 directly targets the NLRP3 ATP-hydrolysis motif for inflammasome inhibition. Nat. Chem. Biol. 15, 556-559. doi:10.1038/s41589-019-0277-7

49. García-Villalba, J., Hurtado-Navarro, L., Peñín-Franch, A., et al. (2022). Soluble P2X7 Receptor Is Elevated in the Plasma of COVID-19 Patients and Correlates With Disease Severity. Front. Immunol. 13, 2207. doi:10.3389/fimmu.2022.894470

50. Ahmad, F., Mishra, N., Ahrenstorf, G., et al. (2018). Evidence of inflammasome activation and formation of monocyte-derived ASC specks in HIV-1 positive patients. AIDS32, 299-307. doi:10.1097/QAD.0000000000001693

51. de Torre-Minguela, C., Barberà-Cremades, M., Gómez, A. I., Martín-Sánchez, F., Pelegrín, P. (2016). Macrophage activation and polarization modify P2X7 receptor secretome influencing the inflammatory process. Sci. Rep. 6, 22586. Doi:10.1038/srep22586

52. Hamarsheh, S., Groß, O., Brummer, T., Zeiser, R. (2020). Immune modulatory effects of oncogenic KRAS in cancer. Nat. Commun. 11, 5439. doi:10.1038/s41467-020-19288-6

53. Niyongere, S., Lucas, N., Zhou, J. M., et al. (2019). Heterogeneous expression of cytokines accounts for clinical diversity and refines prognostication in CMML. Leukemia33, 205-216. doi:10.1038/s41375-018-0203-0

54. Dinarello, C. A., Simon, A., van der Meer, J. W. M. (2012). Treating inflammation by blocking interleukin-1 in a broad spectrum of diseases. Nat. Rev. Drug Discov. 11, 633-652. doi:10.1038/nrd3800

55. Villatoro, A., Cuminetti, V., Bernal, A., et al. (2023). Endogenous IL-1 receptor antagonist restricts healthy and malignant myeloproliferation. Nat. Commun. 14, 12. doi:10.1038/s41467-022-35700-9

56. Teodorovic, L. S., Babolin, C., Rowland, S. L., et al. (2014). Activation of Ras overcomes B-cell tolerance to promote differentiation of autoreactive B cells and production of autoantibodies. Proceedings of the National Academy of Sciences111, E2797-E2806. doi:10.1073/pnas.1402159111

57. Meynier, S., Rieux-Laucat, F. (2019). FAS and RAS related Apoptosis defects: From autoimmunity to leukemia. Immunol. Rev. 287, 50-61. doi:10.1111/imr.12720

58. Andina, N., de Meuron, L., Schnegg-Kaufmann, A. S., et al. (2023). Increased Inflammasome Activation Is Associated with Aging and Chronic Myelomonocytic Leukemia Disease Severity. The Journal of Immunology 210, 580-589. doi:10.4049/jimmunol.2200412

Figure Legends

Figure 1. Evolution of autoinflammatory episodes and levels of IL-1β of CMML *KRAS*^{G12D} patient treated with anakinra.

(**A**) Picture of the cellulitis episode on the lower legs of the index patient.

(**B**) Interleukin-1β release from peripheral blood (PB) mononuclear cells from healthy donors (n=4, each dot represents an independent donor) and the index patient with a *KRAS*^{G12D} mutation before anakinra treatment (each dot represents a technical replicate).

(**C**) Evolution of PB monocytes count during the evolution of the index patient. After introduction of anakinra the patient was free of autoinflammatory episodes for 4 months, after which new episodes of autoinflammation occurred and anakinra was discontinued. Three weeks later constrictive pericarditis with congestive heart failure refractory to all therapeutic measures taken, associated with congestive nephropathy and cryptogenic organized pneumonia, in critical life-threatening condition, anakinra was reintroduced. Note the decrease of monocyte count in response to anakinra treatment (both the first time and when restored).

(**D**) Left orchiepididymitis. Left testicle 27 x 26 x 32 mm in size, with heterogeneous echogenicity. The color Doppler flow is increased. The epididymis is enlarged and vascularized. Diffuse edema of the subcutaneous cellular tissue in the left hemiscrotal. The right testicle is smaller (18 x 26 x 26 mm) and shows a normal vascularization.

(**E**) Computed tomography of the chest with contrast: axial plane (left) and coronal plane (right). *Top* (08/04/2021): Multiple bilateral pseudonodular ground-glass lung opacities associated with bilateral pleural effusion. *Bottom* (20 days later): Bilateral parenchymal involvement with extensive ground glass areas. In the lower left lobe, there was an increase in the radiodensity of the pre-existing opacities with multiple peripheral

consolidations that were not seen in the previous study. Moderate bilateral pleural effusion, which enters through the fissures, has worsened slightly compared to the previous study. Mild pericardial thickening of up to 3 mm.

Figure 2. Anakinra treatment reduces NLRP3 inflammasome activation.

(**A, B**) Release of IL-1β from peripheral blood mononuclear cells (**A**) and percentage of ASC-specking monocytes (**B**), at baseline or after canonical activation of NLRP3 (LPS+ATP) and Pyrin (LPS+TcdB) inflammasome, in the absence/presence of MCC950 from healthy donors (n=2-3, each dot represents an individual donor, white bars) and the index patient with the *KRAS*^{G12D} mutation before anakinra administration (grey bars).

(**C**) Percentage of monocytes with an ASC oligomer from the index patient over the time points examined before and after anakinra treatment.

(**D**) Percentage of monocytes with an ASC oligomer from the index patient after canonical NLRP3 inflammasome activation with LPS+ATP (green) or Pyrin inflammasome activation with LPS+TcdB (dark blue) over the time points examined before and after anakinra treatment.

(**E, F**) Release of IL-1β (**E**), IL-18 (**F**) from peripheral blood mononuclear cells, at baseline or treated, as indicated for NLRP3 (LPS+ATP) or Pyrin (LPS+TcdB) inflammasome canonical activation, in healthy donors (n=3, each dot represents an individual donor, white bars) and the index patient during anakinra treatment (green bars).

(**G**) Plasma levels of ASC in the index patient along the time points examined before and after anakinra treatment.

(**H**) Concentration of IL-1 family cytokines in the plasma of the CMML *KRAS*^{G12D} index patient in response to anakinra.

Data is represented as mean ± SEM and each dot represents an individual donor.

Figure 3. Monocytes from CMML *KRAS*^{mut} patients present a constitutive inflammasome activation.

(**A**) Percentage of ASC-specking monocytes in healthy controls (white bars), CMML patients without *KRAS* mutation (*KRAS*^{wt}, blue bars) and CMML patients with a *KRAS* mutation (*KRAS*^{mut}, orange bars) at baseline or treated as indicated for NLRP3 (LPS+ATP) or Pyrin (LPS+TcdB) inflammasome activation.

(**B, C**) Release of IL-1β from peripheral blood mononuclear cells (**B**) and the formation of ASC-specks in monocytes (**C**) in CMML *KRAS*^{mut} patients at baseline or after the indicated stimulation or treatment (LPS+ATP and LPS+TcdB for NLRP3 or Pyrin inflammasome, respectively), in the absence/presence of MCC950. (**B**) Fold increase was calculated to control non-stimulated conditions, average of the higher value used to calculate fold-increase is 1066.58 pg/ml.

(**D**) Percentage of extracellular LDH from untreated PBMCs from healthy donors (white bar), *KRAS*^{wt} patients (blue bar) and *KRAS*^{mut} patients (orange bar). Data is normalized to the percentage of monocytes.

(**E**) Plasma concentration of HMGB1 and P2X7 receptor from healthy donors (white bar), *KRAS*^{wt} patients (blue bar) and *KRAS*^{mut} patients (orange bar).

Data is represented as mean ± SEM; Each dot represents an individual patient; Ordinary one-way ANOVA test (two-tailed) was used for **A** (* compares CMML *KRAS*^{mut} *vs* healthy controls; † compares CMML *KRAS*^{mut} *vs.* CMML *KRAS*^{wt}), and two-tailed *t*-test in **B**, **C**, **D**, and **E**. Note that * or † $p < 0.05$; **$p < 0.01$; ***$p < 0.001$; **** or †††† $p < 0.0001$; *ns*, no significant difference ($p > 0.05$).

Figure 4. Plasma cytokines in CMML patients.

(**A**) Plasma concentration of IL-1α, IL-1β, IL-1RA, IL-18, IL-12 p40 and IL-12 p70, TNF-α, IL-6 and IL-8. Data is represented as mean ± SEM. Each dot represents an individual patient. Mann-Whitney U test (two-tailed) was used to compare between groups: *KRAS*^{mut} (n=9), and *KRAS*^{wt} patients (n=8); healthy controls (n=9); and patients with sepsis (n=5, as control of acute inflammation). Outliers were detected in the data sets by the Grubbs' test ($\alpha = 0.001$). *$p < 0.05$; **$p < 0.01$; ***$p < 0.001$; ****$p < 0.0001$.

(**B**) Plasma cytokine concentration showing significant differences observed when comparing CMML *KRAS*^{wt} *vs.* healthy controls, CMML *KRAS*^{mut} *vs.* healthy controls and CMML *KRAS*^{mut} *vs.* CMML *KRAS*^{wt} (Volcano plots). X-axis represents log2 (Fold Change) and Y-axis represents the negative log (p-value). Statistically increased (red) was considered when $p < 0.05$ and Fold Change > 1, and statistically decreased (blue) was considered when $p < 0.05$ and Fold Change < 1. Each dot represents a cytokine, and the relevant ones are indicated. IL-2, IL-10 and GM-CSF were not detected in most patients.

Figure 1

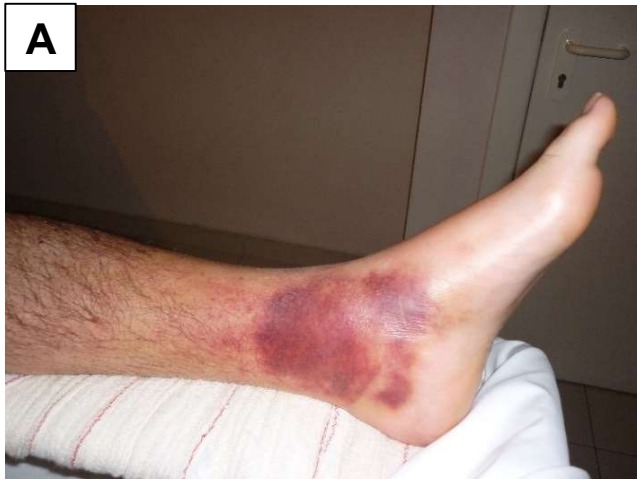
A

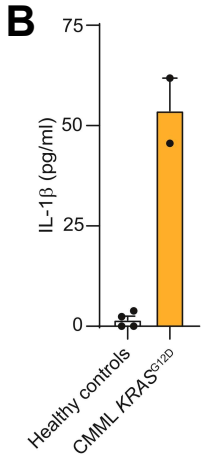
B
75
50
25
0
IL-1β (pg/ml)
Healthy controls
CMML KRAS^{G12D}

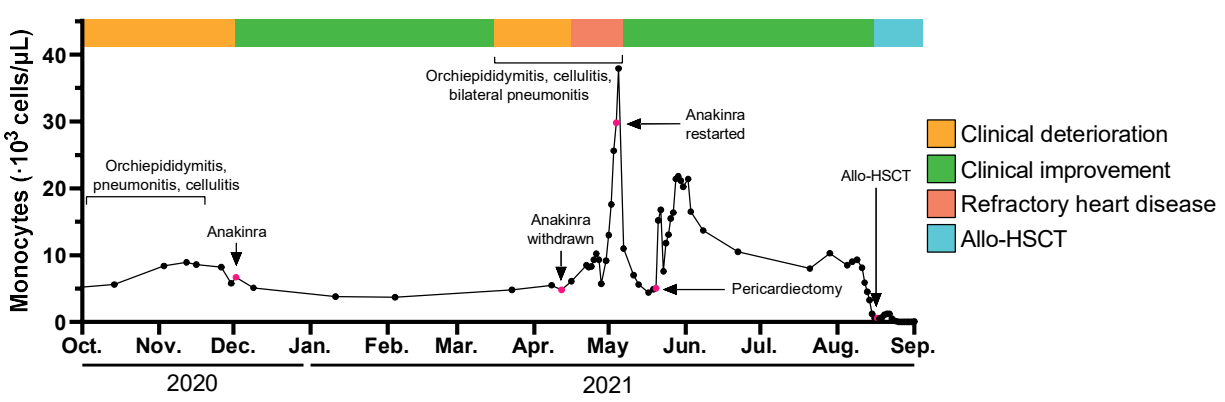
C
Monocytes (·10^3 cells/µL)
40
30
20
10
0
Oct.
Nov.
Dec.
Jan.
Feb.
Mar.
Apr.
May
Jun.
Jul.
Aug.
Sep.
2020
2021
Orchiepididymitis, pneumonitis, cellulitis
Anakinra
Orchiepididymitis, cellulitis, bilateral pneumonitis
Anakinra withdrawn
Anakinra restarted
Pericardiectomy
Allo-HSCT
Clinical deterioration
Clinical improvement
Refractory heart disease
Allo-HSCT

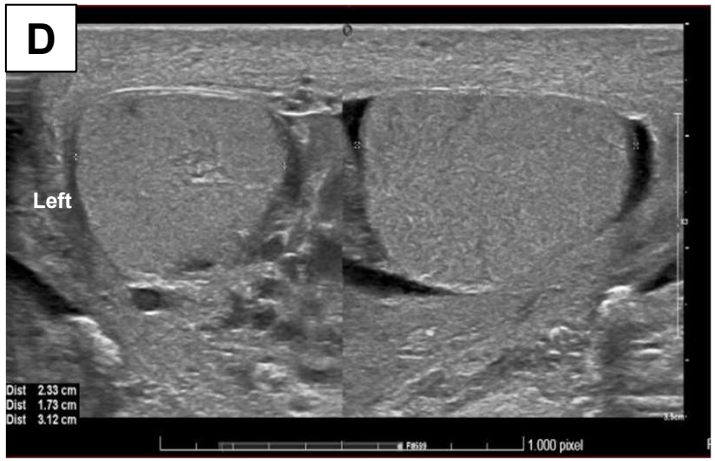
D
Left
Dist 2.33 cm
Dist 1.73 cm
Dist 3.12 cm
1.000 pixel

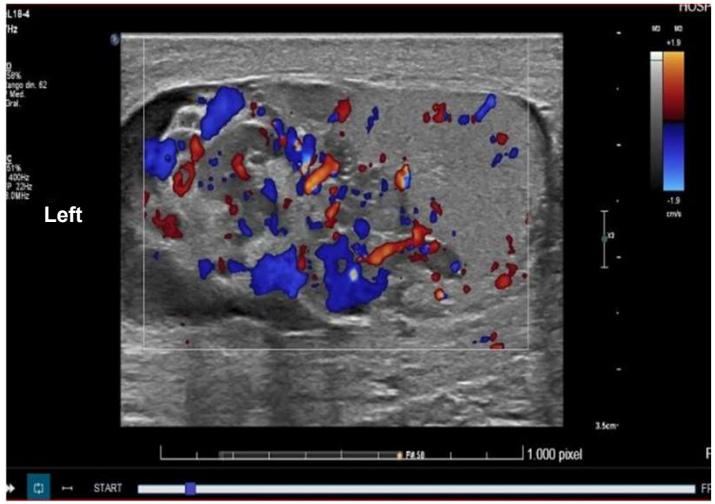
Left
1.000 pixel
START

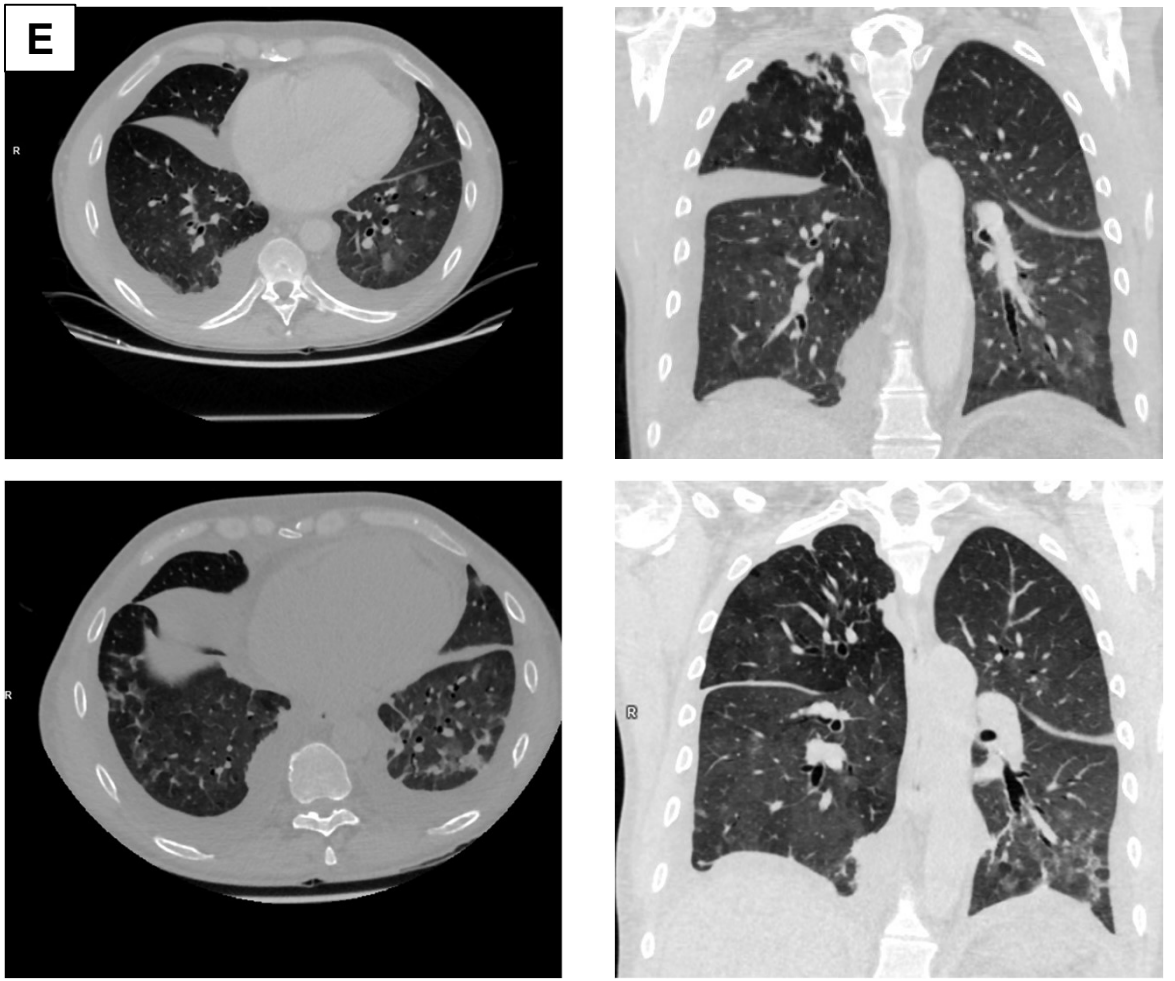
E
R
R

Figure 2

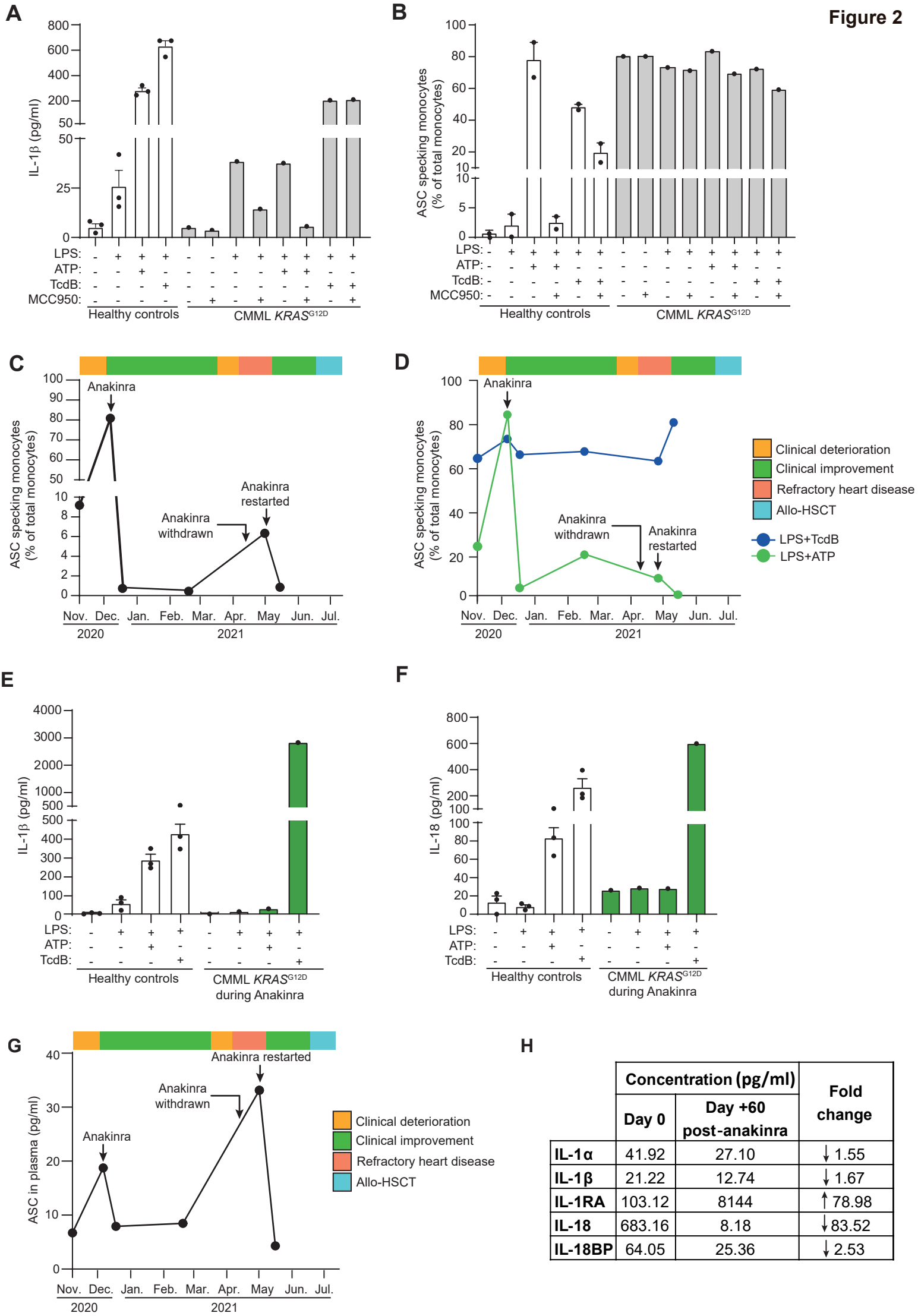

H

	Concentration (pg/ml)		Fold change
	Day 0	Day +60 post-anakinra	
IL-1α	41.92	27.10	↓ 1.55
IL-1β	21.22	12.74	↓ 1.67
IL-1RA	103.12	8144	↑ 78.98
IL-18	683.16	8.18	↓ 83.52
IL-18BP	64.05	25.36	↓ 2.53

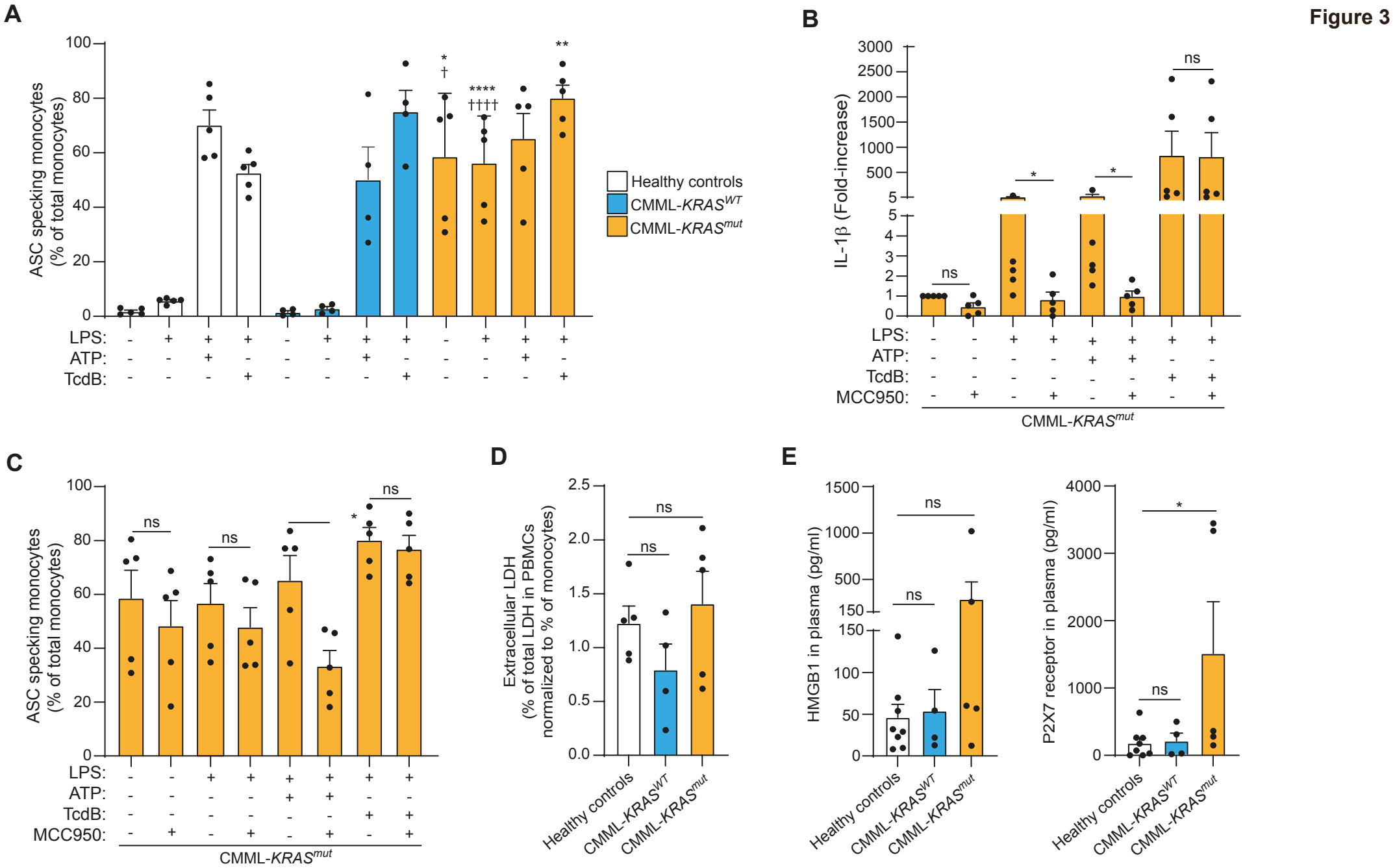
A
ASC specking monocytes (% of total monocytes)
Healthy controls
CMML-KRASWT
CMML-KRASmut
LPS:
ATP:
TcdB:
B
IL-1β (Fold-increase)
MCC950:
CMML-KRASmut
C
ASC specking monocytes (% of total monocytes)
ns
D
Extracellular LDH (% of total LDH in PBMCs normalized to % of monocytes)
E
HMGB1 in plasma (pg/ml)
P2X7 receptor in plasma (pg/ml)

Figure 4

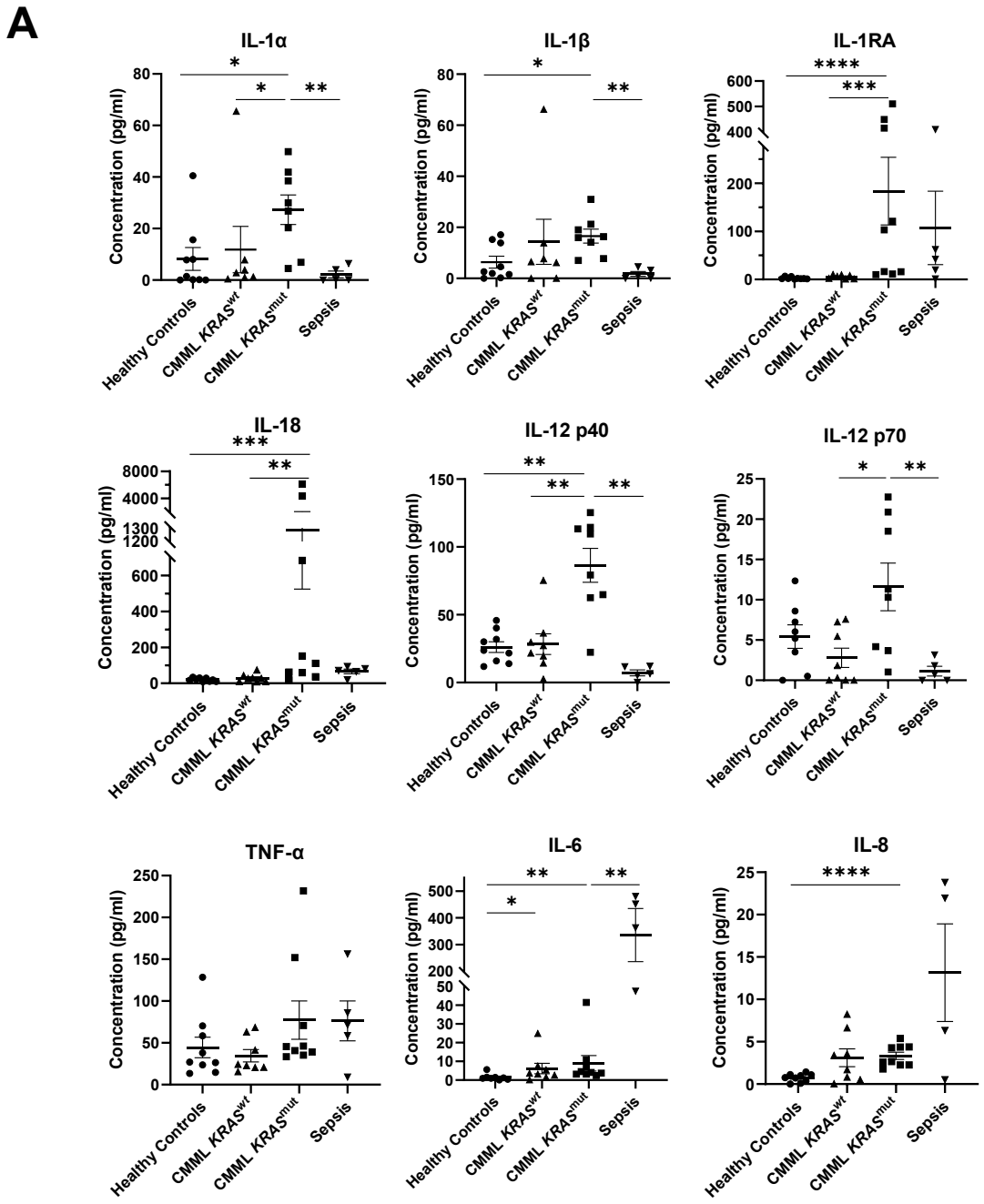
A
IL-1α
IL-1β
IL-1RA
IL-18
IL-12 p40
IL-12 p70
TNF-α
IL-6
IL-8
Concentration (pg/ml)
Healthy Controls
CMML KRASwt
CMML KRASmut
Sepsis

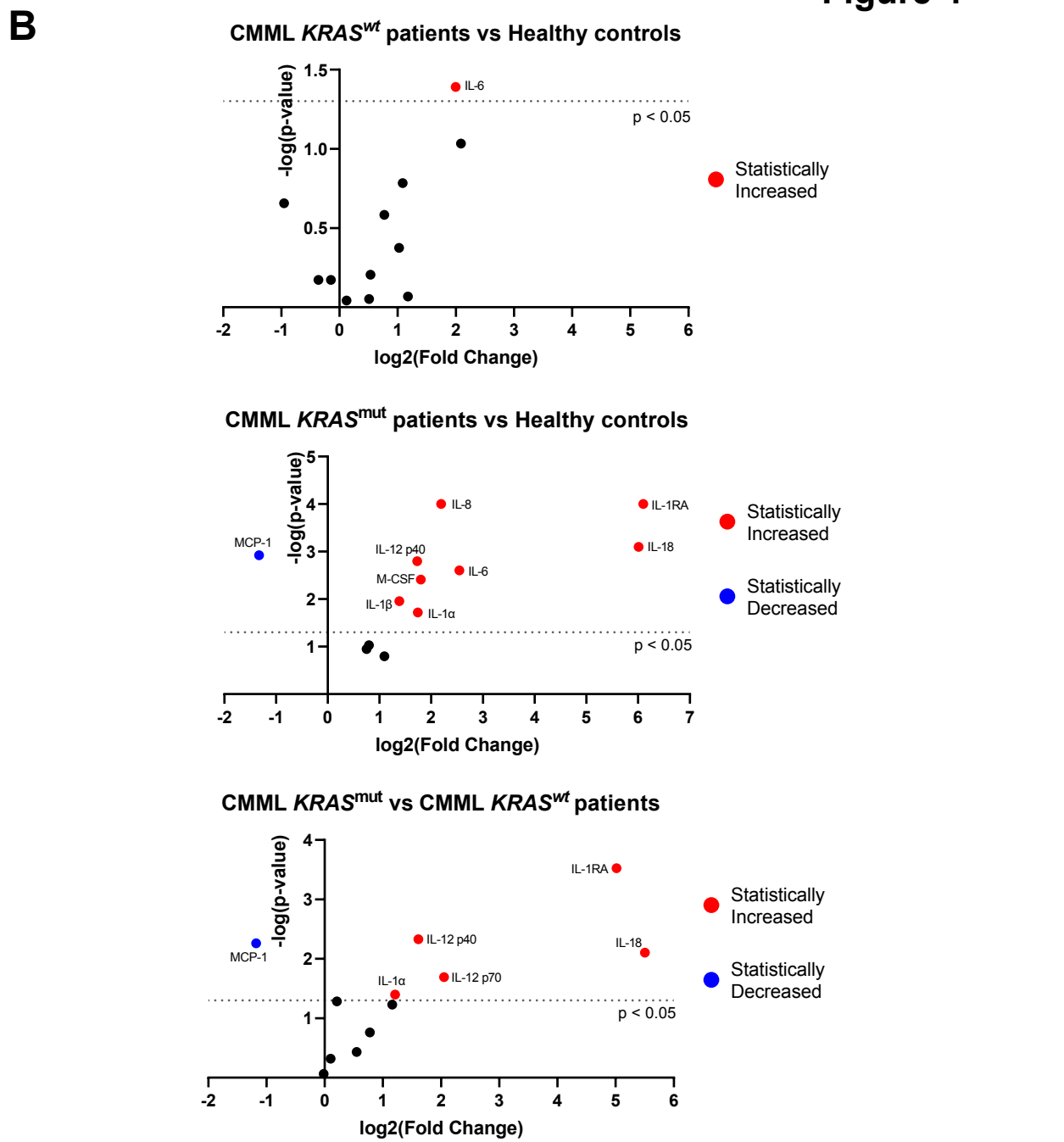
B
CMML KRASwt patients vs Healthy controls
CMML KRASmut patients vs Healthy controls
CMML KRASmut vs CMML KRASwt patients
-log(p-value)
log2(Fold Change)
p < 0.05
IL-6
IL-8
IL-1RA
IL-18
IL-12 p40
M-CSF
IL-1β
IL-1α
MCP-1
IL-12 p70
Statistically Increased
Statistically Decreased

Table S1. Clinical and laboratory features of the CMML *KRAS*^{mut} patient cohort. Related to Figures 1, 2, 3 and 4.

#	Sex	Age (years)	Diagnosis (WHO)	Variant (MP/MD)	*KRAS* (VAF, %)	*NRAS* (VAF, %)	Other gene mutations (VAF, %)	Cytopenias	Monocytes ($\cdot 10^3/\mu l$)	Cytogenetic	autoimmune events; Autoantibodies*	episodes and diagnosis (years)	Progression	Treatment	Exitus If yes, cause	Samples
1	M	54	CMML-2	MP	p.G12D (48.9%)	No	No	A, T	4.5	46,XY	Polyadenitis Effusive-constrictive pericarditis Cellulitis; Orchiepididymitis Bilateral pneumonitis; Pleuritis	6	No	Anakinra HSCT	No	Plasma PB DNA
2	F	47	CMML-1	MP	p.G12D (45.0%)	No	No	A	2.7	46,XX	Pleuropericarditis Polyadenitis Bilateral pneumonitis (x3 episodes) Thrombophlebitis / Cellulitis	4	CMML-1 to CMML-2	EPO	Bilateral pneumonitis	DNA
3	F	67	CMML-1	MD	p.G12D (26.2%)	No	*TET2* (4.00%)	No	1.1	46,XX	ANA	*N/A*	No	Observation	No	Plasma PB DNA
4	F	65	CMML-2	MP	p.G12R (30.9%)	p.G12V (11.9%)	*SRSF2* (42.1%) *ASXL1* (38.4%)	A, T	3.5	46,X,idic(X)(q13)[17]/ 47, idem,+idic(X)(q13)[3]	Polyadenitis RF, ANA, ENA, p-ANCA	0	No	AZA	No	DNA
5	M	58	CMML-2	MP	p.G12D (25.8%)	No	*DNMT3A* (50.4%) *NPM1* (38.7%) *FLT3* , x2 (13.9%; 13.6%) *MTOR* (9.21%)	A, T	6.4	46,XY	No	*N/A*	AML	HU AZA HSCT	COVID-19 bilateral pneumonia	No
6	F	70	CMML-1	MP	p.G12D (39.4%)	No	*WASF3* (51.9%) *NPM1* (20.9%)	A	38	46,XX	No	*N/A*	AML	Observation	AML progression	No
7	M	74	CMML-2	MD	p.G12D (23.4%)	p.G12D (2.15%)	*SF3B1* (31.4%) *GATA2* , x2 (24.3%; 6.94%) *TET2* (10.2%)	A	1.38	46,XY	No	*N/A*	No	AZA	After no response to 5-AZA	No
8	M	30	Unclassifiable MDS/MPN	*N/A*	p.G12D (3.78%)	p.G12D (27.4%)	*NPM1* , x2 (32.6%; 31.0%) *PTPN11* (3.44%)	A	2.57	46,XY	No	*N/A*	No	HDCH HSCT	No	No
9	M	65	CMML-1	MP	p.G12D (44.7%)	No	No	A	9.52	46,XY	Polyadenitis	4	No	EPO	No	Plasma PB DNA
10	F	67	CMML-1	MP	p.G12D (6.39%)	No	*SRSF2* (45.9%) *ASXL1* (38.2%) *KIT* (6.70%)	A	5	46,XX	No	*N/A*	AML	HDCH	AML progression	No
11	F	68	CMML-1	MD	p.G13D (48.0%)	No	No	A, T	3,13	46,XX	Hashimoto's thyroiditis Hashimoto's encephalopathy Rosai-Dorfman disease	10	No	Observation	No	Plasma PB DNA
12	F	65	CMML-1	MD	p.G13D (35.0%)	No	No	A, T	1.0	46,XX	Autoimmune hypothyroidism Immune thrombocytopenia	11	No	Observation	No	No
13	M	75	CMML-1	MP	p.G12R (43.3%)	No	*SRSF2* (46.8%) *IDH2* (45.2%) *ASXL1* (36.9%)	ND	ND	46,XY	ND	ND	No	EPO	No	Plasma
14	F	72	CMML-1	MD	p.G12R (38.8%)	No	No	No	1.9	46,XX	ND	ND	No	Observation	No	Plasma PB DNA
15	M	69	CMML-1	MD	p.G12R (12.9%) p.G60D (2.32%)	p.G12D (15.1%) p.G12V (15.1%) p.Y64D (4.90%)	*TET2* , x2 (3.9%; 2.2%) *JAK2* (2.7%) *CBL* (2.5%)	A, T	1.04	45,X, -Y[20]	Immune thrombocytopenia	0	No	Eltrombopag	Respiratory failure, COPD flare-up	Plasma
16	F	69	CMML-1	MD	p.V14I (19.2%)	No	*ASXL1* , x2 (47.3%; 30.8%) *TET2* , x4 (47.2%; 25.1%; 14.7%; 2.8%) *TP53* (11.2%) *JAK2* (3.30%)	No	1.2	46,XX	No	*N/A*	AML	Observation	AML progression	Plasma
17	F	76	CMML-2	MD	p.G12D (30.8%)	No	*SRSF2* (37.7%) *RUNX1* (5.50%)	A, T	2.27	47,XX,del(20)(q11q13), +21	Polymyalgia rheumatica	0	AML	AZA	AML progression	No
18	M	59	CMML-2	MP	p.G12C (47.2%)	No	No	A, T	10.1	45,XY,-7	ND	ND	No	AZA HSCT	No	Plasma DNA
19	F	68	CMML-1	MP	p.G12D (4.90%)	p.G12D (37.7%)	*TET2* , x2 (41.1%; 40.3%)	T	12.3	ND	Hypothyroidism	4	No	Observation	No	No

Sex (**M:** Male; **F:** Female); **N/A**: Not applicable; **ND**: Not determined; **CMML**: Chronic myelomonocytic leukemia; **MDS**: Myelodysplastic syndrome; **MPN**: Myeloproliferative neoplasm; **MP**: Myeloproliferative; **MD**: Myelodysplastic; **A**: Anemia; **T**: Thrombocytopenia; **RF**: Rheumatoid Factor; **ANA**: Antinuclear antibodies; **ENA**: Extractable nuclear antigen antibodies; **p-ANCA**: Perinuclear antineutrophil cytoplasmic autoantibodies; **AML**: Acute myeloid leukemia; **HSCT**: Hematopoietic Stem Cell Transplant; **EPO**: Erythropoietin; **AZA**: Azacitidine; **HU**: Hydroxyurea; **HDCH**: High Dose Chemotherapy; **COPD**: Chronic obstructive pulmonary disease; **PB**: Peripheral blood

*Autoantibodies were available in 7 patients: #1, 3, 4, 11, 12, 15 and 17.

Table S2. Clinical-biological characteristics of the cohort of CMML and MDS/MPN *KRAS*^{mut} patients (*n*=19). Related to Figures 1, 2, 3 and 4.

Clinical characteristics			
Median age (range) 67 (30-75)			
Females (%)	11/19 (57.9)	Males (%)	8/19 (42.1)
Diagnostic (according to WHO criteria at diagnosis)			
Unclassifiable MDS/MPN (%) 1/19 (5.3)			
CMML (%) 18/19 (94.7)			
CMML-1* (%)	12/18 (66.7)	CMML-MP (%)	10/18 (55.6)
CMML-2* (%)	6/18 (33.3)	CMML-MD (%)	8/18 (44.4)
Cytogenetic			
Available cytogenetic (%) 18/19 (94.7)			
Low risk (%)	15/18 (83.3)	Intermediate/high risk (%)	3/18 (16.7)
Molecular studies			
***Nº (%) of patients with KRAS* mutations**		19 (100) (20 mutations)	
KRAS p.G12D (%)	11/19 (57.9)	*KRAS* p.G12C (%)	1/19 (5.3)
KRAS p.G12R (%)	4/19 (21.1)	*KRAS* p.V14I (%)	1/19 (5.3)
KRAS p.G13D (%)	2/19 (10.5)	*KRAS* p.G60D (%)	1/19 (5.3)
***Nº (%) of patients with NRAS* mutations**		5 (26.3) (7 mutations)	
NRAS p.G12D (%)	4/19 (21.1)	*NRAS* p.Y64D (%)	1/19 (5.3)
NRAS p.G12V (%)	2/19 (10.5)		
***Nº (%) of patients with* mutations in other myeloid genes**		12 (63.2) (30 mutations)	
TET2 mutations (%)	5/19 (26.3)	*IDH2* mutations (%)	1/19 (5.3)
SRSF2 mutations (%)	4/19 (21.1)	*KIT* mutations (%)	1/19 (5.3)
ASXL1 mutations (%)	4/19 (21.1)	*MTOR* mutations (%)	1/19 (5.3)
NPM1 mutations (%)	3/19 (15.8)	*PTPN11* mutations (%)	1/19 (5.3)
JAK2 mutations (%)	2/19 (10.5)	*RUNX1* mutations (%)	1/19 (5.3)
CBL mutations (%)	1/19 (5.3)	*SF3B1* mutations (%)	1/19 (5.3)
DNMT3A mutations (%)	1/19 (5.3)	*TP53* mutations (%)	1/19 (5.3)
FLT3 mutations (%)	1/19 (5.3)	*WASF3* mutations (%)	1/19 (5.3)
GATA2 mutations (%)	1/19 (5.3)		
Autoinflammation			
Patients 10/19 (52.6)			
Adenitis (%)	5/19 (26.3)	Pneumonitis Pleuropericarditis Cellulitis	2/19 (10.5)
Thyroid diseases (%)	3/19 (15.8)		
Treatment (%) 12/19 (63.2)			
Hypomethylating and/or cytoreductive agents (%)	5/19 (26.3)	EPO or TPO stimulating agents (%)	4/19 (21.1)
High-dose CT (%)	2/19 (10.5)	Anakinra (%)	1/19 (5.3)
Allo-HSCT (%) 4/19 (21.1)			
Death (%). 8/19 (42.1)			
Disease progression (%)	5/19 (26.3)	†Respiratory Insufficiency	3/19 (15.8)

WHO: World Health Organization; MDS: myelodysplastic syndromes; MPN: myeloproliferative neoplasms; CMML: chronic myelomonocytic leukemia; MP: myeloproliferative; MD: myelodysplastic; EPO: erythropoietin; TPO: thrombopoietin; CT: chemotherapy; Allo-HSCT: Allogeneic Hematopoietic Stem Cell Transplant; * According to the percentage of blasts and promonocytes in BM and PB. † Respiratory insufficiency (#2, 5, 15, 1 by COVID-19, and 1 due to bilateral autoinflammatory pneumonitis).

Table S3. Clinical and laboratory features of the CMML *KRAS*^{wt} patient cohort. Related to Figures 3 and 4.

#	Sex	Age (years)	Diagnosis (WHO)	Variant (MP/MD)	RAS mutations		Other gene mutations (VAF, %)	Cytopenias	Monocytes ($\cdot 10^3/\mu l$)	Cytogenetic	Autoinflammatory or autoimmune events; Autoantibodies	Time between episodes and diagnosis (years)	Progression	Treatment	Exitus If yes, cause	Samples
					KRAS (VAF, %)	NRAS (VAF, %)										
20	M	68	CMML-1	MD	No	No	*TET2* (44.5%), *TET2* (45.6%), *SRSF2* (37.9%)	A, T	3.6	46,XY	No	*N/A*	No	AZA	No	PB Plasma DNA
21	F	88	CMML-1	MP	No	No	*ASXL1* (42.1%)	A	3	46,XX	No	*N/A*	Hematological progression	HU	Hematological progression	PB Plasma DNA
22	M	53	CMML-2	MD	No	No	*TET2* (88.9%), *ZRSR2* (88.3%)	A	2.2	46,XY	ANA	7	No	Observation	No	Plasma DNA
23	F	82	CMML-2	MD	No	No	*TET2* (46.8%), *TET2* (46.8%), *SRSF2* (44.6%)	A, T	1.6	46,XX	Primary Sjögren's syndrome	0	No	AZA	Subarachnoid hemorrhage	Plasma DNA
24	M	47	CMML-1	MP	No	No	No	No	1	46,XY	No	*N/A*	No	Observation	No	Plasma DNA
25	F	75	CMML-1	MD	No	No	*DNMT3A* (49.3%), *IDH2* (47.5%), *SRSF2* (42.2%)	A, T	1.5	46,XX	No	*N/A*	AML	AZA	Hematological progression	Plasma DNA
26	F	69	CMML-1	MD	No	No	*TET2*(25%) *RUNX1*(31.7%) *DNMT3A* (28.3%)	A, T	2.3	46,XX	No	*N/A*	AML	AZA	Hematological progression	Plasma DNA
27	M	79	CMML-2	MD	No	No	*IDH1* (41.3%)	A	2.2	46,XY	No	*N/A*	No	Observation	Oncological complications	Plasma DNA
28	M	61	CMML-1	MD	No	No	*DNMT3A* (39.8%), *TET2* (38.3%), *IDH1* (16.2%)	T	1	46,XY, der(1;7)(q10;p10) [13]/46,XY[7]	No	*N/A*	No	Observation	No	PB DNA
29	M	75	CMML-1	MD	No	No	*TET2* (88.4%), *ZRSR2* (84.3%)	A	1	45,X0, -Y [20]	No	*N/A*	Hematological progression	AZA	Hematological progression	PB DNA

Sex (M: Male; F: Female); CMML: Chronic myelomonocytic leukemia; MD: Myelodysplastic; MP: Myeloproliferative; VAF: Variant allele frequency; A: Anemia; T: Thrombocytopenia; ANA: Antinuclear antibodies; *N/A:* Not applicable; AML: Acute myeloid leukemia; AZA: azacytidine; HU: hydroxyurea; PB: Peripheral blood.

Table S4. List of genes involved in inflammasome-related diseases that have been used to filter the results obtained by whole exome sequencing. Related to Figure 3.

Inflammasome	*NLRP3, NLRC4, PYCARD, AIM2, NLRP1, NLRP7, NLRP2, CASP1, CASP5, CASP4, CARD8, IL1B, IL18, IL1A, IL1R1, NEK7, NOD1, NOD2, TXNIP, MEFV, RHOA, HMGB1, FADD, TNFR1, PYRIN*
Purinergic receptors	*PANX1, P2RX4, P2RX6, P2RX2, P2RX5, P2RX3, P2RX1, P2RX7, P2RY2*
Gasdermines	*GSDMD, GSDMA, GSDMC, GSDMB, PJVK*
Necroptosis	*RIPK1, RIPK3, CASP8, TLR3, TNF, MLKL, AMD1* TLR-like receptors: *TLR1, TLR2, TLR4, TLR6*
Others	*MYD88, CD14, CD16, IL23, IL33, IL10, IL6, CRP*

Table S5. Plasma cytokine levels measured by Luminex in each of the groups tested and statistical analysis. Related to Figure 4.

	Cytokines concentration in pg/mL											
	Healthy Control		CMML *KRAS*^{wt}		p-value[a]	CMML *KRAS*^{mut}		p-value[b]	p-value[c]	Sepsis		p-value[d]
	Range	Mean ± SEM	Range	Mean ± SEM		Range	Mean ± SEM			Range	Mean ± SEM	
IL-1α	0.00 – 40.48	8.19 ± 4.42	0.43 – 65.48	11.83 ± 8.99	ns	4.47 – 49.83	27.33 ± 5.73	*	*	0.00 – 6.42	2.18 ± 1.30	**
IL-1β	0.01 – 17.10	6.36 ± 2.32	0.00 – 66.21	14.35 ± 8.83	ns	7.03 – 30.96	16.57 ± 2.70	*	ns	0.00 – 4.59	1.77 ± 0.91	**
IL-1RA	0.69 – 7.01	2.68 ± 0.76	0.95 – 10.54	5.68 ± 1.54	ns	9.96 – 510.1	183.6 ± 70.41	****	***	1.22 – 408.4	107.0 ± 76.34	ns
IL-12 p40	11.86 – 45.84	26.12 ± 3.94	2.62 – 75.35	28.36 ± 7.63	ns	22.35 – 125.3	86.45 ± 12.49	**	**	0.14 – 12.02	7.15 ± 2.21	**
IL-12 p70	0.00 – 12.35	5.43 ± 1.46	0.00 – 7.57	2.80 ± 1.20	ns	1.03 – 22.77	11.58 ± 2.96	ns	*	0.00 – 3.16	1.14 ± 0.61	**
IL-18	9.64 – 33.60	20.00 ± 3.00	8.25 – 74.46	28.41 ± 7.85	ns	18.54 – 6123	1287 ± 762.8	***	**	19.06 – 93.46	66.21 ± 12.70	ns
IL-6	0.04 – 5.64	1.54 ± 0.61	0.16 – 24.89	6.14 ± 2.80	*	2.41 – 41.47	8.97 ± 4.16	**	ns	47.48 – 480.3	335.6 ± 99.25	**
IL-8	0.00 – 1.42	0.73 ± 0.16	0.03 – 8.24	3.11 ± 1.06	ns	1.79 – 5.38	3.33 ± 0.42	****	ns	0.52 – 23.80	13.15 ± 5.75	ns
TNF-α	13.53 – 128.5	44.51 ± 12.29	15.42 – 68.50	34.57 ± 7.33	ns	33.41 – 231.7	77.18 ± 22.95	ns	ns	8.96 – 156.4	76.28 ± 23.85	ns
IL-15	3.05 – 9.91	5.96 ± 0.86	0.12 – 24.48	10.15 ± 3.12	ns	4.01 – 17.36	10.01 ± 2.03	ns	ns	2.43 – 32.63	14.44 ± 4.96	ns
MCP-1	82.07 – 276.70	137.5 ± 19.95	47.52 – 239.6	123.9 ± 20.65	ns	20.79 – 116.2	54.67 ± 10.53	**	**	175.9 – 521.3	359.8 ± 70.86	**
M-CSF	0.00 – 130.2	38.22 ± 15.15	0.00 – 211.7	77.63 ± 32.61	ns	12.48 – 207.2	132.8 ± 21.30	**	ns	77.19 – 567.2	333.8 ± 100.4	ns

Results are shown as range and mean± standard error of the mean (SEM).
[a] Mann-Whitney U test (two-tailed), Healthy control vsCMML *KRAS*^{wt}
[b] Mann-Whitney U test (two-tailed), Healthy control vsCMML *KRAS*^{mut}
[c] Mann-Whitney U test (two-tailed), CMML *KRAS*^{wt} vs CMML *KRAS*^{mut}
[d] Mann-Whitney U test (two-tailed), CMML *KRAS*^{mut} vs Sepsis
ns: not significant, *: $p < 0.05$, **: $p < 0.01$, ***: $p < 0.001$, ****: $p < 0.0001$

Table S6. Plasma cytokine levels measured in CMML patients by Luminex according to other genetic and/or biological parameters, and statistical analysis. Related to Figure 4.

Genetic parameters			
	***TET2* mutations**		
	Yes (n=7)	**No (n=10)**	**p-value**
IL-1α (mean±SEM)	204 ± 113.20	15.42 ± 5.07	ns
IL-1RA (mean±SEM)	28.11 ± 18.73	152.30 ± 67.76	ns
IL-12 p40 (mean±SEM)	62.95 ± 14.76	53.09 ± 14.89	ns
IL-12 p70 (mean±SEM)	5.86 ± 2.78	7.99 ± 2.65	ns
IL-18 (mean±SEM)	42.13 ± 12.95	1151 ± 695.50	ns
	***SRSF2* mutations**		
	Yes (n=4)	**No (n=13)**	**p-value**
IL-1α (mean±SEM)	172.50 ± 165	23.24 ± 6.34	ns
IL-1RA (mean±SEM)	380.40 ± 252.60	95.35 ± 46.73	ns
IL-12 p40 (mean±SEM)	53.54 ± 25.49	58.69 ± 11.55	ns
IL-12 p70 (mean±SEM)	4.39 ± 2.61	8.13 ± 2.39	ns
IL-18 (mean±SEM)	35.20 ± 11.47	897.40 ± 545	ns
	***ASXL1* mutations**		
	Yes (n=3)	**No (n=14)**	**p-value**
IL-1α (mean ± SEM)	15.81 ± 7.92	109.60 ± 60.40	ns
IL-1RA (mean ± SEM)	154 ± 147.60	164.20 ± 82	ns
IL-12 p40 (mean ± SEM)	64.51 ± 28.93	55.76 ± 11.40	ns
IL-12 p70 (mean ± SEM)	10.21 ± 4.81	6.49 ± 2.13	ns
IL-18 (mean ± SEM)	29.96 ± 16.37	836.90 ± 508.10	ns
Biological parameters			
	CMML subtype		
	MP (n=6)	**MD (n=11)**	**p-value**
IL-1α (mean ± SEM)	16.65 ± 6.91	134.80 ± 75.80	ns
IL-1RA (mean ± SEM)	248.10 ± 95.90	20.38 ± 11.32	ns
IL-12 p40 (mean ± SEM)	69.27 ± 22.15	52.01 ± 11.55	ns
IL-12 p70 (mean ± SEM)	9.66 ± 3.01	5.71 ± 2.47	ns
IL-18 (mean ± SEM)	1874 ± 1091	51.41 ± 13.57	ns

MP: Myeloproliferative; MD: Myelodysplastic; ns: not significant

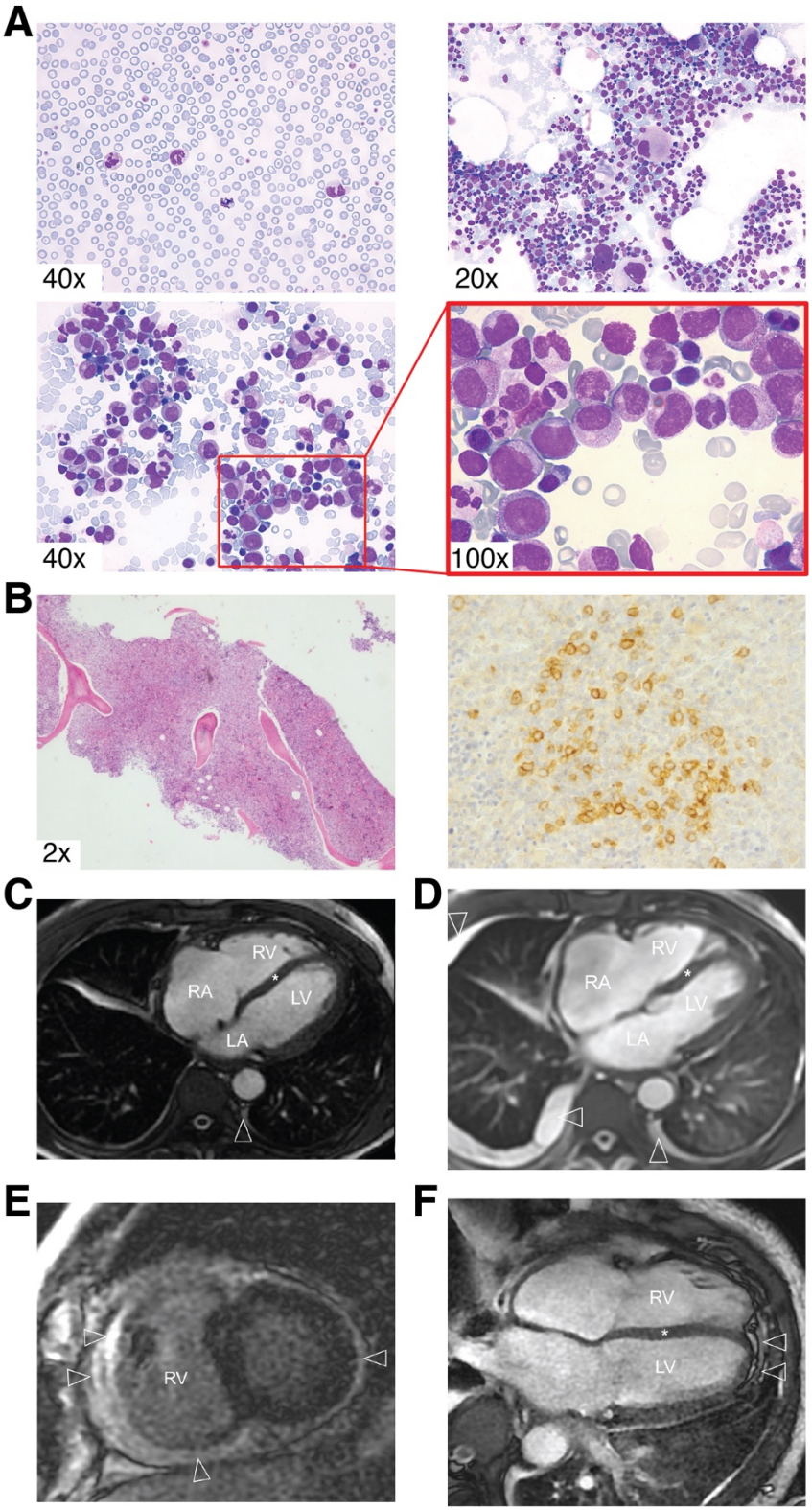

Figure S1. Cytomorphological and histologic findings, at diagnosis, in peripheral blood (PB) and bone marrow (BM) in the CMML *KRAS*^{G12D} index patient, and cardiac magnetic resonance imaging. Related to Figure 1.

(**A**) Cytologic examination of PB and BM aspirates. Findings in PB (*Upper left*, 40x magnification): monocytosis (atypical monocytes); anisopoikilocytosis, and platelet macrodysmorphia. Hematoxylin and eosin (H&E)-stained BM aspirate: *Upper right*, 20x; *Lower left*, 40x. Note the dysplastic features and the expansion of immature elements between myeloblasts, monoblasts and promonocytes. Detail at higher magnification (*lower right*, 100x).

(**B**) Histologic examination of BM biopsy. *Left*, 2x: H&E staining. The BM is markedly hypercellular. *Right*: immunohistochemistry, CD123 stain. CD123 positive cell clusters, which are commonly described in the BM of patients with CMML.

(**C, D**) Pure axial plane white blood cine steady-state free precession (SSFP) type magnetic resonance imaging (MRI) sequences with a difference of 8 months (A: July 2020; B: March 2021). Tubular morphology of both ventricles, dilatation of both atria, verticalization of the interventricular septum (*), findings in the context of ventricular filling restriction due to pericardial constriction, and bilateral pleural effusion (arrowheads). The pleural effusion has increased in extent on the most current study.

(**E**) Late enhancement MRI sequence in short axis plane (March 2021): diffuse enhancement of the two pericardial leaflets (arrowheads), more evident in the region adjacent to the right ventricle.

(**F**) White-blood SSFP cine MRI sequence in 4-chamber view (March 2021): tubular morphology of both ventricles secondary to pericardial constriction, with flattening of the interventricular septum (*) in the same context; pericardial thickening (arrowhead) not accompanied by pericardial effusion is also identified.

Abbreviations: LA (left atrium), RA (right atrium), RV (right ventricle), LV (left ventricle)

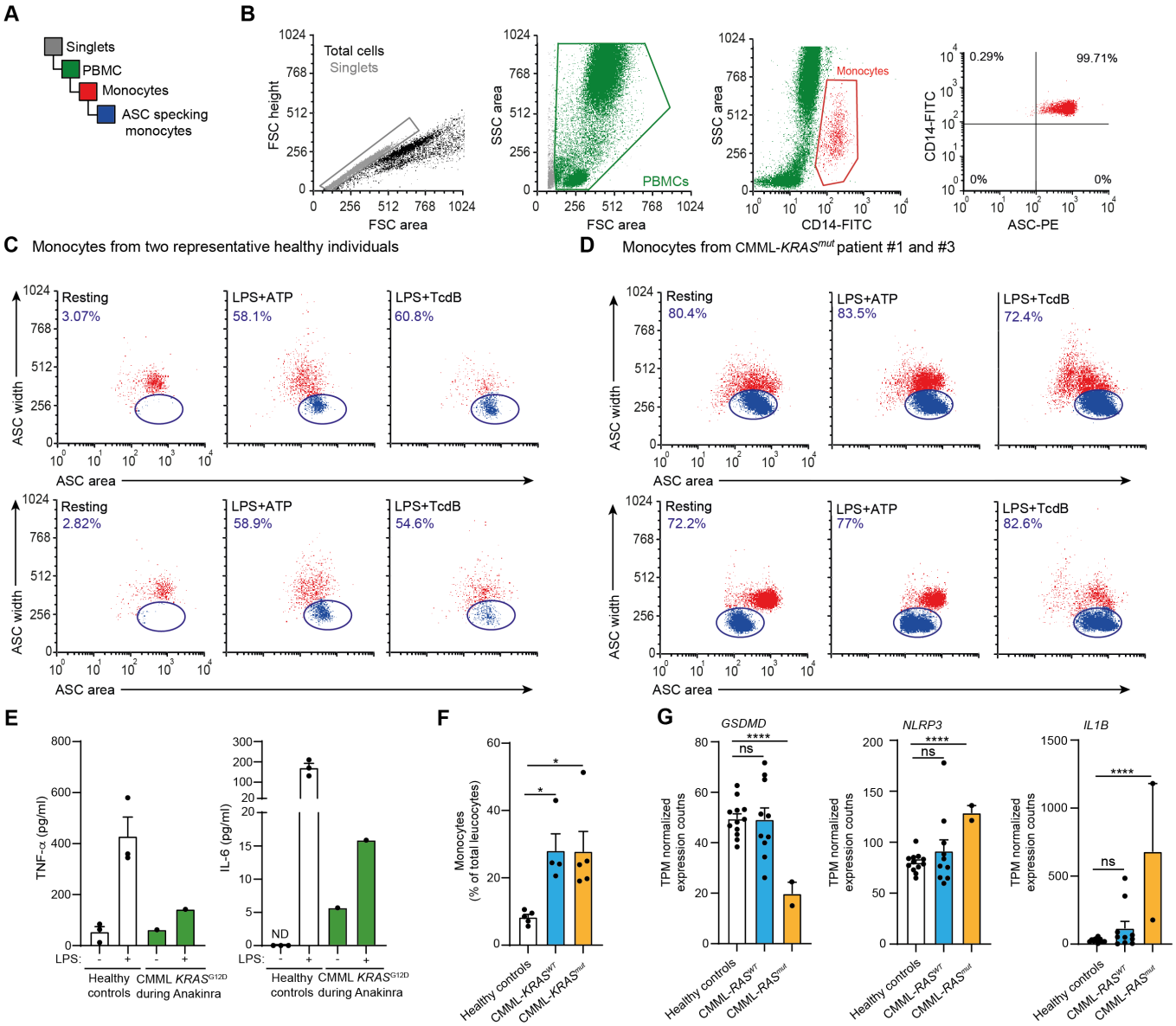

Figure S2. Gating strategy to identify monocytes with ASC specks, and release of cytokines, percentage of monocytes from healthy donors and CMML patients, as well as omnibus data gene expression. Related to Figures 2 and 3.

(**A**) Populations hierarchy analyzed in flow cytometry experiments to determine ASC specking monocytes.

(**B**) Peripheral blood mononuclear cells (PBMCs) were gated from total cells obtained after Ficoll isolation selecting singlet cells in a forward scatter (FSC) height vs area dot plot and then excluding cell debris in a FSC vs side scatter (SSC) dot plot. Monocytes were gated from PBMCs by the positive staining with an anti-CD14 FITC monoclonal antibody in a SSC vs CD14 FITC dot plot. ASC positive monocytes (>95%) were gated by the positive staining with an anti-CD14 FITC and anti-ASC PE monoclonal antibodies in a CD14 FITC vs ASC PE dot plot.

(**C,D**) Time of flight inflammasome evaluation showing the quantification of ASC specking monocytes obtained from two representative healthy controls (**C**) and two representative CMML-*KRAS*^{mut} patients (#1 and #3) (**D**). ASC specking monocytes were gated based in an ASC PE-width vs ASC PE-area dot plots after priming or not of the cells with LPS (1.6 mg/ml) during 2 h and then stimulated with ATP (3 mM) for 15 min or with TcdB (1 mg/ml) for 30 min.

(**E**) TNF-α and IL-6 cytokine concentrations in the supernatants of LPS-treated peripheral blood mononuclear cells from healthy donors (n=3, each dot represents an individual donor, white bars) and the CMML *KRAS*^{mut} index patient (#1) during anakinra treatment (green bars). Data is represented as mean ± SEM. ND: not detected.

(**F**) Percentage of monocytes from the total of blood leukocytes from healthy donors, CMML *KRAS*^{wt} patients and *KRAS*^{mut} patients.

(**G**) Expression of *GSDMD*, *NLRP3* and *IL1B* in whole blood cells of healthy donors, CMML patients with *RAS*^{wt} and *RAS*^{mut}. Data analyzed from omnibus data GSE13590.